4th User Meeting at the FRM II
March 23rd, 2012 - Garching

www.frm2.tum.de

Imprint

Dear colleagues,

this 4th User Meeting is organised in close proximity to the restart of the FRM II and we are very pleased that more than 100 participants registered for this event. In 2010 our first long maintenance break started on October 21st and had lasted for more than one year. Today most of the instruments are back to work and we are happy to welcome our users in Garching.

For our user meeting, due to the limitation of a single day, only a few of the submitted abstracts could be chosen for oral presentation. Their topics cover different areas of science performed at the FRM II: From small angle scattering and soft matter to ultra-cold neutrons and to several aspects of material science. All this is only possible because of your ideas, proposals and experiments! Therefore we appreciate very much your engagement at the FRM II and the use of the still growing suite of instruments operated by our partners of German universities and research institutes.

There are a lot of news this time: Most of the instrument teams seized the opportunity of the long maintenance break to upgrade their instruments. Other instruments are now ready for users, like MARIA and BIODIFF. Please find all instrument posters in the second part so you do not miss anything! The first part of the posters is dedicated to Science & Projects and shows the whole range of neutron scattering applications. In addition, planned instruments as well as the sample environment groups and software development are presented. And first of all we are looking forward to many interesting and stimulating discussions with both our colleagues from abroad and from the Garching campus.

In 2011 we have started a closer cooperation between the TUM and institutes of the Helmholtz association, i.e. the German neutron sources in Berlin and formerly in Jülich and Geesthacht. This cooperation is based on additional funding from the BMBF to strengthen the scientific use of the FRM II. It is a permanent task for us to improve our service and infrastructure for performing neutron experiments in Garching. Feedback from you is therefor highly appreciated. Especially for the performance of the sample environment and to identify future needs of our users, we have launched a survey on our web server on which we would like to draw your intention. Please visit our web site and participate on this survey at

www.frm2.tum.de/user-office/userumfrage-probenumgebung

Enjoy the day at the User Meeting and don't miss the next deadline for proposals on July 20th, 2012!

Flavio Carsughi
User Office
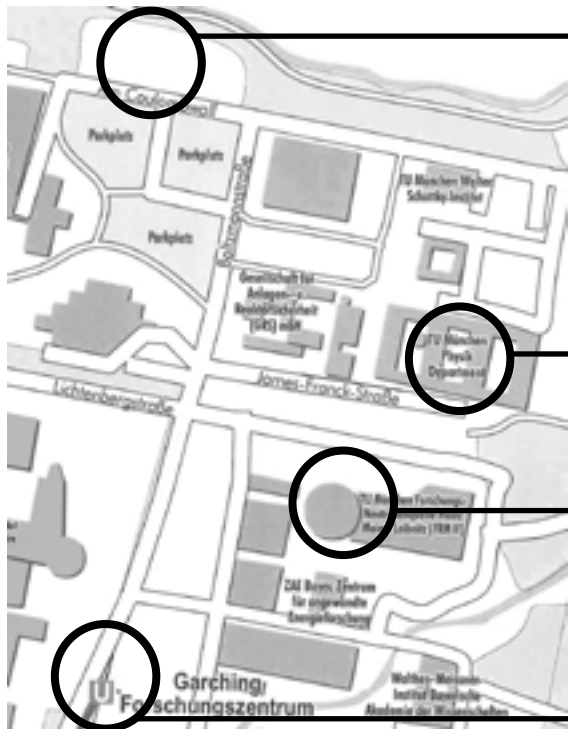
Parking

Venue:
Technische Universität München
Physik Department
James Franck Str.
85748 Garching

- Lecture hall: HS3 -

FRM II

Underground: U6,
"Garching, Forschungszentrum"

Public transportation

The **U6** takes you to the city centre. The timetable (right) tells you when a train leaves at „Garching, Forschungszentrum". The timeline (above) informs you how long it will take to reach a station (in minutes).

User Office

In case you need other timetables, please contact the User Office. It is a mobile one today. In case you need help or have any questions, there will always be someone in front of the lecture hall to assist you.

Apart from that you can call **+49 (0)89.289.10794**

Uhr	Freitag					
5	11	31	51			
6	11	23	33	43	53	
7	03	13	23	33	43	53
8	03	13	23	33	43	53
9	03	13	23	33	43*	53
10	03*	13	33	53		
11	13	33	53			
12	13	33	53			
13	13	23	33	43	53	
14	03	13	23	33	43	53
15	03	13	23	33	43	53
16	03	13	23	33	43	53
17	03	13	23	33	43	53
18	03	13	23	33	43	53
19	13	33	51			
20	11	31	51			
21	11	31	51			
22	11	31	51			
23	11	31	51			
0	11	31				
1	01	46*				
2	46*					

Venue

PH II ↑

Posters

Catering

Registration

WC
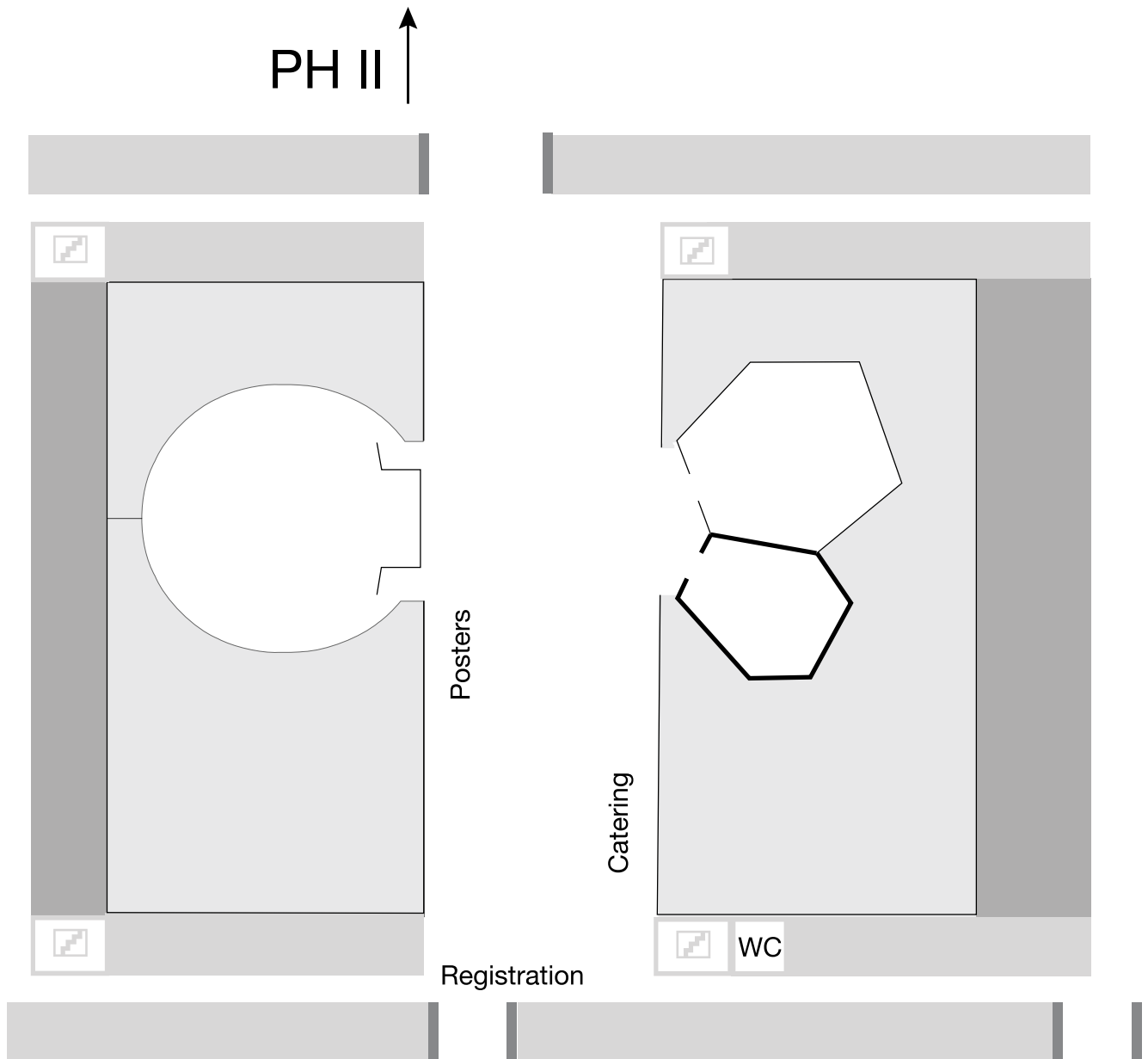
Technische Universität München
Physik Department
James-Franck-Straße 1
85748 Garching

Lecture hall HS3

Programme

09:15-09:45	Coffee and registration
09:45-10:00	Welcome

10:00-10:20	**T-01** - Henrich Frielinghaus, JCNS Dynamics of microemulsions adjacent to planar walls
10:20-10:40	**T-02** - Ivan Krakovský, Charles University Prague SANS study of structural changes in epoxy hydrogels induced by external stimuli
10:40-1:00	**T-03** - Peter Müller-Buschbaum, TUM Polymer nanostructures at buried interfaces probed with time-of-flight grazing incidence small angle neutron scattering
11:00-11:20	**T-04** - Felix Roosen-Runge, Universität Tübingen Hydration and interactions in protein solutions containing concentrated electrolytes studied by small-angle scattering
11:20-11:40	**T-05** - Bert Nickel, LMU Interaction of α-synuclein with lipid membranes
11:40-12:00	**T-06** - Marco Zanatta, Università di Trento High frequency dynamics in glassy SiSe2
12:00-13:30	Lunch

13:30-14:00	**T-07** - Andreas Frei, FRM II The ultra-cold neutron laboratory at the FRM II
14:00-14:20	**T-08** - Georg Brandl, FRM II Large scales - long times: Adding high energy resolution to SANS
14:20-14:40	**T-09** - Amitesh Paul, TUM Vertical correlation of domains due to non-collinear and out-of-plane exchange coupling
14:40-15:00	**T-10** - Béla Nagy, Wigner Research Centre Magnetic proximity at the superconductor-ferromagnet interface studied by waveguide-enhanced polarized neutron reflectometry
15:00-15:30	Coffeebreak

15:30-15:50	**T-11** - Zsolt Révay, FRM II Standardization of low-cross-section nuclides
15:50-16:10	**T-12** - James Rolph, University of Manchester Residual stress evolution through manufacture of sub-scale turbine discs
16:10-16:30	**T-13** - Pavel Strunz, NPI Rež Stability and evolution of phases in Co-Re-base alloys during high-temperature exposure
16:30-16:45	Conclusion
16:45-17:00	Conference photo
17:00-19:00	Postersession

Talks

Dynamics of microemulsions adjacent to planar walls

H. Frielinghaus[1], F. Lipfert[2], M. Kerscher[2], O. Holderer[1], D. Richter[1,2]

[1]Jülich Centre for Neutron Science, Garching, Germany
[2]Forschungszentrum Jülich GmbH, Institute for Complex Systems 1, Jülich, Germany

In the enhanced oil recovery aqueous surfactant systems are frequently used for secondary/tertiary oil recovery and fracturing fluids. In the first case the fluid viscosity needs to be similar to the oil in order to drive the oil towards the borehole without fingering, i.e. bypassing. The viscosity of the fracturing fluid also needs to be high in order to deposit the pressure energy in the sand stone for crack generation. The proppant consists of simple sand particles, which keep the cracks from collapsing after the application. The highly porous sand stone allows for a faster oil exploration. The fluid in contact with oil forms microemulsions with a low viscosity. Currently, we study microemulsions as model systems in the presence of planar hydrophilic surfaces. Recently [1], we have developed and successfully applied the method of grazing incidence neutron spin echo spectroscopy (GINSES) to microemulsions adjacent to hydrophilic walls. While grazing incidence scattering methods aim at surface near structures, the combination with neutron spin echo spectroscopy allows for studying the dynamics. This means reducing the irradiated volume by huge factors, while microemulsions themselves scatter strongly.

The structure of the microemulsion was characterized by neutron reflectometry and grazing incidence small angle neutron scattering (GISANS) [2]. Especially, GISANS allows for a depth resolved structural characterization. The bulk structure is bicontinuous, while the near surface structure is lamellar. Two perfect double layers (water-surfactant-oil-surfactant) are formed before the ordered structure decays gradually into the volume. The results are supported by computer simulations.

The spectroscopy reveals depth resolved information about the dynamics of the surfactant membranes. The near surface membranes are found to be three times faster than in the bulk. The explanation is supported by the application of the Seifert theory for confined membranes to the Zilman-Granek theory for the dynamics of fluctuating membranes. While the membranes in the bulk fluctuate with modes limited by the patch size – a typical size where the orientation of the membrane is maintained – the lamellar ordered membranes have additional long wavelength modes. These modes are considerably faster compared to the bulk dispersion relation due to the wall reflections of the hydrodynamic modes, and they strongly contribute to the observed GINSES relaxation times.

The faster kinetics support the picture of lubrication for induced lamellar order adjacent to planar walls. This in itself is important for microemulsions in surface dominated flow fields, for instance in enhanced oil recovery.

[1] H. Frielinghaus, M. Kerscher, O. Holderer, M. Monkenbusch, D. Richter, Phys. Rev. Lett. (submitted 2011)
[2] M. Kerscher, P. Busch, S. Mattauch, H. Frielinghaus, D. Richter, M. Belushkin, G. Gompper, Phys. Rev. E 83, 030401 (2011)

SANS study of structural changes in epoxy hydrogels induced by external stimuli

I. Krakovský[1], N. Székely[2,3]

[1]Charles University, Faculty of Mathematics and Physics, Department of Macromolecular Physics, Prague, Czech Republic
[2]Budapest Neutron Centre, Research Institute for Solid State Physics and Optics, Budapest, Hungary
[3]Jülich Centre for Neutron Science, Garching, Germany

Two stoichiometric epoxy networks were prepared by end-linking reaction of α,ω-diamino terminated poly(oxypropylene) -b-poly(oxyethylene)-b-poly(oxypropylene) (POP-POE-POP) Jeffamine ED600 (number average of molar mass: M_n = ca 600 g/mol) and ED2003(M_n = ca 2000 g/mol) with diglycidyl ether of Bisphenol A propoxylate (PDGEBA). The first network (of higher crosslinking density and lower content of hydrophilic POE) was swollen to equilibrium in solutions of HCl in D_2O. Significant effect of the presence of D_3O^+ formed by dissociation of HCl in D_2O on the swelling degree and structure of resulting hydrogels is observed (Fig. 1a). In agreement to our previous studies of epoxy hydrogels [1,2], the hydrogel structure is nanophase separated and consists of water -rich and water-poor domains. Characteristic length of nanophase separation as estimated using Bragg distance, $D_B = 2\pi/q_{max}$, (q_{max} is the position of scattering peak) yields value ca 50 Å. Position of the scattering peak does not change with concentration of HCl, at least in the range of concentrations investigated. However, the intensity of peak grows reflecting increasing degree of nanophase separation induced by the presence of D_3O^+ ions. This can be attributed to charging of epoxy network (be means of nitrogen atoms in amino groups) as well as changes of polymer -water interaction due to perturbation of hydrogen-bonded structure of water by D_3O^+ ions.

The second network (of lower crosslinking density and higher content of h ydrophilic POE) was swollen in solutions of a surfactant (sodium dodecylsulphate(SDDS)) in D_2O. Effect of surfactant concentration on swelling degree and nanophase separated structure of hydrogels is shown in Fig. 1b . A distinct scattering peak is observed in all hydrogels. With increasing concentration of surfactant, the scattering peak shifts to higher q-values and its intensity decreases. This corresponds to changes of Bragg distance from ca 90 Å (in D_2O) to 65 Å (0.1 M SDDS/D_2O). These changes can be attributed to a compatibilisation effect of the surfactant on hydrophobic and hydrophilic parts of the system.

Interestingly, the scattering curves in both systems investigated intersect in single point (isosbesticpoint). We have observed the same phenomenon in our previous studies of hydrogels and explained it by conservation of Porod length of inhomogeneity [3].

[1] I. Krakovský, J. Pleštil, L. Almásy: Polymer 47, 218-226 (2006)
[2] I. Krakovský, N.K.Székely: J.Non-Cryst. Solids 356, 368-373 (2010)
[3] I. Krakovský, N.K. Székely: Eur. Polym. J., 47, 2177-2188 (2011)
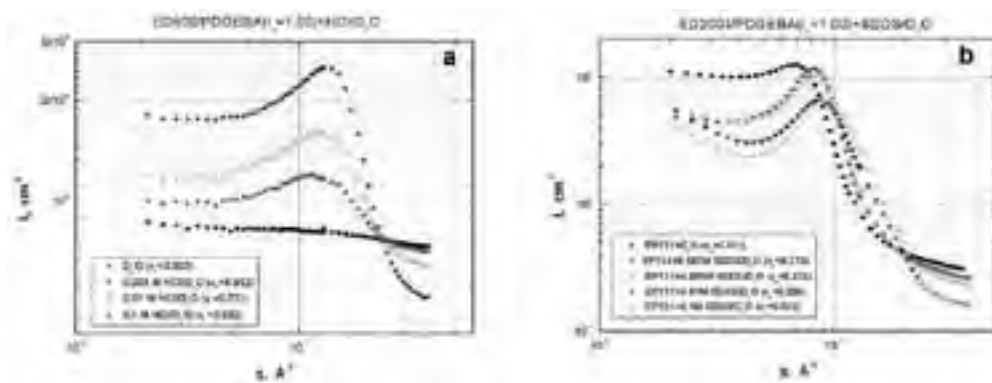
Fig.1: SANS scattering profiles obtained from the epoxy networks swollen to equilibrium in solutions of HCl (a) and SDDS (b) in D_2O at 25°C. $r_s = 2[NH_2]_0/[E]_0$ denotes stoichiometric ratio (initial ratio of amino and epoxy groups), v_p denotes polymer volume fraction in swollen networks (swelling degree).

Polymer nanostructures at buried interfaces probed witnn time-of flight grazing incidence small angle neutron scattering

P. Müller-Buschbaum[1], E. Metwalli[1], J.-F. Moulin[2], M. Haese-Seiller[2], R. Kampmann[2]

[1]TUM, Physik Department, Garching, Germany
[2]Helmholtz Zentrum Geesthacht, Outstation at FRM II, Garching, Germany

Nano-structured polymer materials have multiple applications in many technological areas. Thus, self-organizing block copolymers continue to receive strong attention due to their ability to spontaneously form such ordered nanostructures. These nanostructures result from a competition between repulsive interactions (enthalpic) and chain packing (entropic), and are sensitive to molecular design parameters such as monomer incompatibility, molecular weight, monomer asymmetry and composition. Of the many copolymer architectures studied, most work has concentrated on simple di-block copolymers built from immiscible monomer units (A and B). In AB-type di-block copolymers a rich variety of different structures ranging from spheres to cylinders to lamellae and to a more complex bi-continuous cubic phase have been reported. As compared to bulk morphologies, at interfaces the interaction with the confining wall modifies the morphologies. A preferential selectivity of one wall starts to order the ABtype di-block copolymer thereby yielding an alignment of the structures parallel to this interface. In contrast, the behavior of thick copolymer films is more complex. The powderlike oriented lamellar structure in the bulk becomes oriented along the surface normal in the vicinity of the substrate [1]. A modification of the short-ranged interface potential of the substrate introduces a stretching of the lateral spacing of this lamellar structure up to 8 % as compared to the bulk [2].

Difficulties in probing such structuring of buried interfaces are overcome with grazing incidence small angle neutron scattering (GISANS). With GISANS high interface sensitivity is reached and a depth profiling is accessible [3]. Time-of flight (TOF) mode allows for a specular and off-specular scattering experiment, in which neutrons with a broad range of wavelengths are used simultaneously and recorded as a function of their respective times of flight. The combination of both, TOF-GISANS, enables the simultaneous performance of several GISANS measurements, which differ in wavelength [4]. As a consequence, within one measurement a full set of GISANS pattern related to different scattering vectors, different scattering depths and resolutions result, which allows the detection of nanostructures with a chemical sensitivity.

We demonstrate the potential of TOF-GISANS to access lateral structures at buried interfaces and to obtain a depth resolution in the model system of microphase separation induced nanostructures in AB-type di-block copolymer films.

[1] P. Müller-Buschbaum, E. Maurer, E. Bauer, R. Cubitt; Langmuir 22, 9295 (2006)
[2] P. Müller-Buschbaum, L. Schulz, E. Metwalli, J.-F. Moulin, R. Cubitt; Langmuir, 24, 7639-7644 (2008)
[3] P. Müller-Buschbaum, L. Schulz, E. Metwalli, J.-F. Moulin, R. Cubitt; Langmuir 25, 4235-4242 (2009)
[4] P. Müller-Buschbaum, E. Metwalli, J.-F. Moulin, V. Kudryashov, M. Haese-Seiller, R. Kampmann; Euro. Phys. J. E ST. 167, 107-112 (2009)

Hydration and interactions in protein solutions containing concentrated electrolytes studied by small-angle scattering

F. Zhang[1], F. Roosen-Runge[1], M. W. A. Skoda[2], R. M. J. Jacobs[3], M. Wolf[1], P. Callow[4], H. Frielinghaus[5], V. Pipich[5], S. Prévost[6], F. Schreiber[1]

[1] Eberhard Karls Universität Tübingen, Institut für Angewandte Physik, Germany

[2] STFC ISIS, Rutherford Appleton Laboratory, Chilton, Didcot, United Kingdom

[3] University of Oxford, Department of Chemistry, Chemistry Research Laboratory, United Kingdom

[4] Institut Laue-Langevin, Grenoble, France

[5] Jülich Centre for Neutron Science, Garching, Germany

[6] Helmholtz-Zentrum Berlin, Germany

During protein crystallization and purification, proteins are commonly found in concentrated salt solutions. Although of practical relevance, protein interactions under these conditions are far from being understood, in particular when considering the interplay of hydration and salt ions. Here, we present a study on a model globular protein (bovine serum albumin, BSA) in concentrated salt solutions by small-angle neutron and X-ray scattering (SANS and SAXS).[1] The comparison of SAXS and SANS reveals a considerable difference in apparent volume (Fig.1).

For SANS, we obtain an averaged molecular volume for BSA of 91 700 A^3, which is about 37% smaller than that determined by SAXS, corresponding to a hydration level of 0.30 g water/g protein. From the forward intensity I(0) we determine the second virial coefficient,

A_2, which describes the overall protein interactions in solution (Fig. 2a). It is found that A^2 follows the reverse order of the Hofmeister series, i.e. $(NH_4)_2SO_4 <$ $Na_2SO_4 < NaOAc < NaCl < NaNO_3 < NaSCN$ (Fig.2(b)). The dimensionless second virial coefficient B_2 is calculated to allow conclusions on the overall interaction. Using the results from the experimental structure factor as a benchmark, corrections for hydration shell and the non-spherical shape of the protein are found necessary to give a consistent description of protein interactions.

[1] F. Zhang, F. Roosen-Runge, M.W.A. Skoda, R.M.J. Jacobs, M. Wolf, P. Callow, H. Frielinghaus, V. Pipich, S. Prévost and F. Schreiber, Phys. Chem. Chem. Phys., 14 (2012), 2483-2493
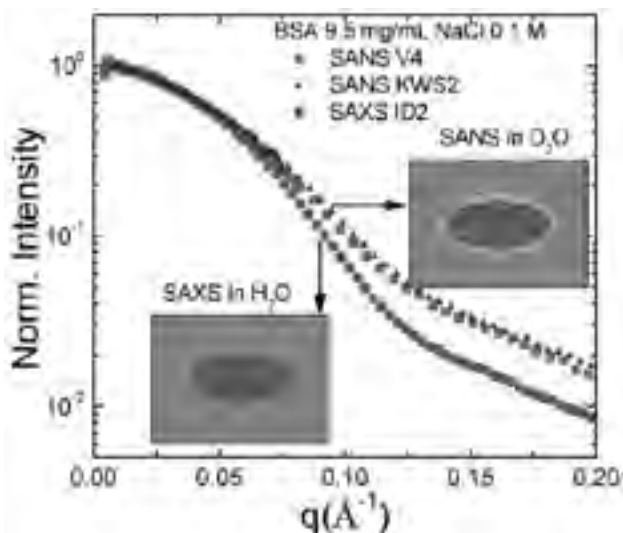
Fig.1: Form factor for BSA in dilute solutions for SANS and SAXS. The difference indicates a different apparent volume, which is attributed to the hydration shell. (Figure taken from [1])
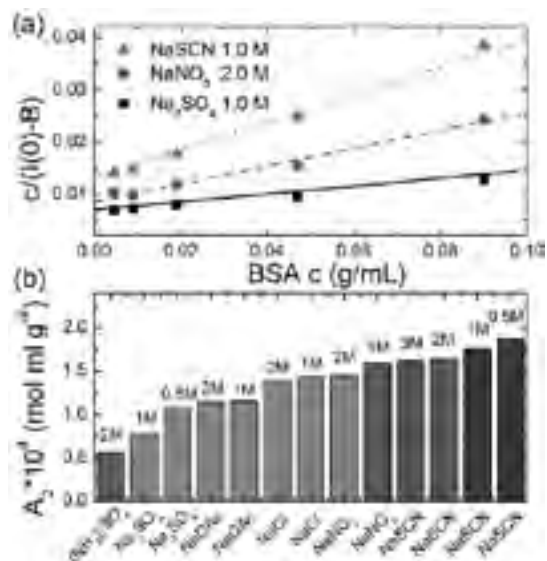
Fig.2: (a) Determination of A_2 from the low-q scattering I(0). (b) The second virial coefficients A_2 follow the reverse order of the Hofmeister series. (Figure taken from [1])

Interaction of α-synuclein with lipid membranes

J. Schmidt[1], S. Hertrich[1], B. Nickel[1], J. Rädler[1], F. Kamp[2], J-F. Moulin[3]

[1]LMU, Fakultät für Physik & CeNS, München, Germany
[2]LMU, Deutsches Zentrum für Neurodegenerative Erkrankungen, München, Germany
[3]Helmholtz-Zentrum Geesthacht, Outstation at FRM II, Garching, Germany

The interaction of proteins with lipid membranes is a key component in the complex regulation of signal transduction and cellular behavior. In the case of α-synuclein, the binding involves a change in conformation from random coil in solution to a helical shape in the membrane bound state. Beyond these two conformations, α-synuclein, a major pathogen in Parkinson's disease, exhibits a third conformation which favors the formation of large protein aggregates (Lewy bodies). Here, we report the influence of α-synuclein binding on the structure and fluidity of the membrane it binds to. The reflectometry experiments are performed at REFSANS. We observe a reduction of bilayer thickness upon binding of α-synuclein. Furthermore, we report first results from GISANS experiments at lipid vesicles.
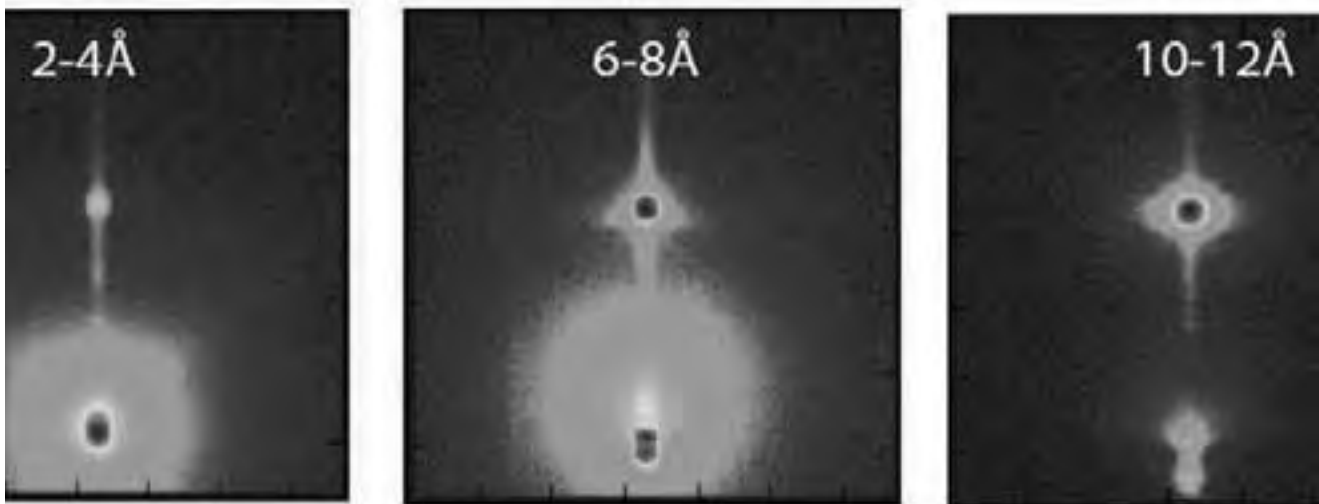
Fig.1: GISANS data from lipid vesicles (diameter 100 nm) adsorbed to a SiO$_2$ surface.

High frequency dynamics in glassy SiSe$_2$

M. Zanatta[1]

[1]Università di Trento, Italy

We present an inelastic neutron scattering investigation of the vibrational dynamics of glassy SiSe$_2$. This system is characterized by a rather low sound velocity which matches very well with the kinematic range of an inelastic neutron scattering experiment.

To describe the relevant dynamic features we have performed two experiments using different neutron spectrometers. The wide dynamic range BRISP spectrometer at the Institut Laue Langevin (Grenoble, France) has been used for a general survey of the dynamic structure factor S(Q,ω) whereas the TOFTOF spectrometer at FRM II (Munich, Germany) has provided the proper resolution to enhance the low energy features which are quite close to the very strong elastic peak.

The dynamic structure factor shows three excitations. The high frequency mode presents a pseudo-periodic behavior and it can be associated to the highfrequency counterpart of the longitudinal acoustic mode. Conversely the low frequency modes are more intriguing since their characters are not obvious and they are located around the boson peak energy.

The Ultra-Cold Neutron laboratory at the FRM II

A. Frei[1], P. Fierlinger[2], S. Paul[2], W. Petry[1], R. Stoepler[2]

[1]Forschungs-Neutronenquelle Heinz Maier-Leibnitz (FRM II), Garching, Germany
[2]TUM, Physik Department, Garching, Germany

Ultra-Cold Neutrons (UCN) are, due to their intrinsic properties, well suited particles for experiments, investigating fundamental properties of the free neutron with highest precision. Such experiments search e.g. for an electric dipole moment (EDM) of the neutron, for quantum effects of neutrons in the earth magnetic field, or try to determine the lifetime τ_n of the free neutron and the axial vector coupling constant g_A of the weak interaction. At the FRM II a laboratory for experiments with UCN is currently under construction. The UCN-source, feeding such experiments, will be installed in the trough-going horizontal beam tube SR6.

The UCN converter, consisting of solid ortho-deuterium and a solid hydrogen premoderator, will produce UCN according to the superthermal principle, which are then extracted out of the converter and guided to the various experiments. This poster will give an overview of the current status of the UCN-source and of planned experiments. The UCN-laboratory is supported by the DFG cluster of excellence EXC153 "Origin and Structure of the Universe", and by the Maier-Leibnitz-Laboratorium (MLL) of the Universität München and the Technische Universität München.

Large scales - long times: adding high energy resolution to SANS

<u>G. Brandl</u>[1,2], R. Georgii[1,2], W. Häußler[1,2], S. Mühlbauer[3], P. Böni[2]

[1]Forschungsneutronenquelle Heinz Maier Leibnitz (FRM II), Garching, Germany
[2]TUM, Physik Department, Garching, Germany
[3]ETH Zürich, Laboratorium für Festkörperphysik, Switzerland

The Neutron Spin Echo (NSE) variant MIEZE (Modulation of IntEnsity by Zero Effort), where all beam manipulations are performed before the sample position, offers the possibility to perform low background SANS measurements in strong magnetic fields and depolarising samples. However, MIEZE is sensitive to differences ΔL in the length of neutron flight paths through the instrument and the sample.

Here, we discuss the major influence of ΔL on contrast reduction of MIEZE measurements and its minimisation. Finally we present a design case for enhancing a small-angle neutron scattering (SANS) instrument at the planned European Spallation Source (ESS) in Lund, Sweden, using a combination of MIEZE and other TOF options, such as TISANE offering time windows from ns to minutes.

The proposed instrument would allow obtaining an excellent energyand Q-resolution straightforward to µs for 0.01 Å, even in magnetic fields, depolarising samples as they occur in soft matter and magnetism while keeping the instrumental effort and costs low.

Vertical correlation of domains due to non-collinear and out-of-plane exchange-coupling

A. Paul[1,2], N. Paul[2], S. Mattauch[3]

[a]TUM, Physik Department, Garching, Germany
[b]Helmholtz-Zentrum Berlin, Germany
[c]Jülich Centre for Neutron Science, Garching, Germany

Conventionally, magnetization is probed along the plane of the exchange biased direction in an exchange coupled ferromagnet-antiferromagnetic (FM-AF) system. The exchange bias direction (unidirectional anisotropy) can be in-plane or out-of-plane of the sample, as the AF uniaxial anisotropy can lie either along the exchange anisotropy direction or can be in any direction in the sample plane. In such cases, where the magnetization is probed perpendicular to the exchange anisotropy direction, the system typically shows a hard-axis-type behavior. However, with polarized neutron scattering measurements at TREFF (Fig.1), we show that competing anisotropic directions can not only change the magnetization behavior in an out-of-plane unidirectional anisotropic system but also can effectively bring in magnetic correlation of domains (in-plane and out-of-plane) [1]. Note that these domains were vertically uncorrelated for a conventional (in-plane unidirectional anisotropic) case [2].

[1] A. Paul, New J. Phys., 13, 063008, (2011).
[2] A. Paul, Appl. Phys. Lett. 97, 032505 (2010).
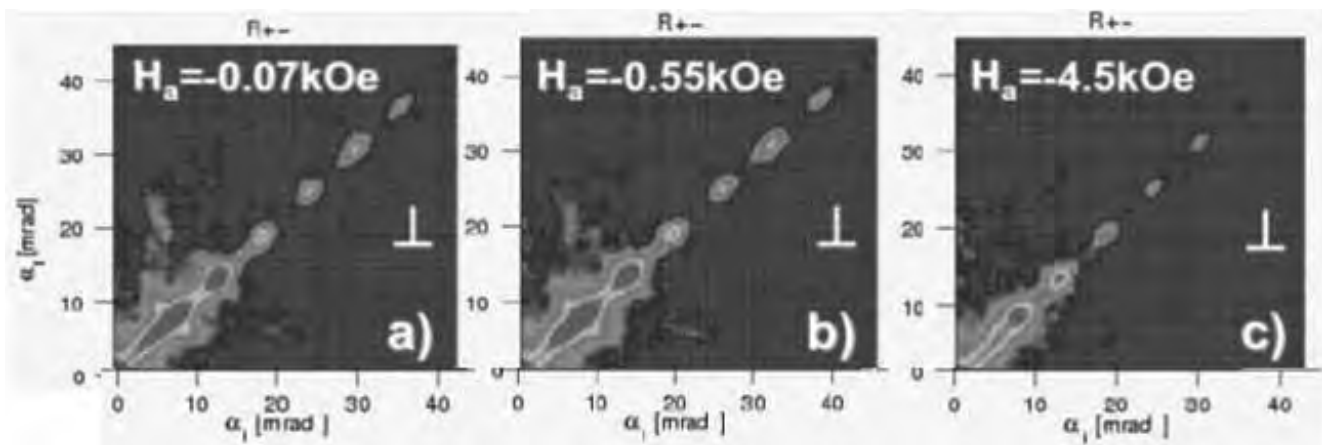
Fig.1: SF intensity maps [R−+] from Co/CoO/Au ML with perpendicular field cooling (inducing outof- plane unidirectional anisotropy) and measured at different applied fields (a–c) along the first half of the first field cycle. The scattered intensities, showing vertical correlation of domains (as Bragg sheets), are plotted on a logarithmic scale for incident angle a_i and exit angle α_f. The Bragg sheets gradually disappear with an increase in the applied field strength indicating their magnetic origin.

Magnetic proximity at the superconductor-ferromagnet interface studied by waveguide-enhanced polarized neutron reflectometry

B. Nagy[1], N. Khaydukov[2], L. Bottyán[1]

[1]Wigner Centre for Physics, Budapest, Hungary

[2]Max Planck Institute for Solid State Research, Stuttgart, Germany

A ferromagnet (F) and singlet superconductor (S) represent mutually exclusive microscopic electron correlations in the solid state however macroscopically coexist in the region of a F/S interface. Extensive recent theoretical work has been exerted to understand the nature of these mixed states [1].

The S/F interaction is rather weak and the mixed region is relatively thin (of the order of the electron correlation length of the superconductor) therefore experimental studies of F/S bilayer systems have been sparse. The thin layer structure and the magnetic character of the problem make polarized neutron reflectometry (PNR) an ideal tool for studying S/F bilayers, however the required sensitivity can only be achieved by multiple layers [2] or by applying a novel tool, waveguide enhancement [3] by placing the S/F interface in a neutron resonator structure. Pilot experiment on such Fe/V layer system revealed an induced magnetization in the V layer parallel with the magnetization of the Fe layer [4]. Theory predicts an oscillating dependence of the induced magnetization upon the product of the layer thickness and the exchange coupling strength of the F layer [5].

Here we present an extended study of the magnetic proximity effect in V/F bilayers in neutron waveguide resonator structures with ferromagnetic layers (Fe, Co, Ni) of different exchange coupling strength and different hickness. Reflectivity curves in all four spin channels were recorded at multiple temperatures above and below the superconducting critical temperature. From the change of the width of the resonance one can conclude if the induced magnetization is positive or negative. An example of V/Ni(3nm) is shown in Fig.1.

[1] A. I. Buzdin, Reviews of Modern Physics, 77, 935 (2005)

[2] J. Stahn, J. Chakhalian, Ch. Niedermayer, J. Hoppler, T. Gutberlet, J. Voigt, F. Treubel, H-U. Habermeier, G. Cristiani, B. Keimer, and C. Bernhard, Phys. Rev. B 71, 140509(R) (2005)

[3] Yu.N. Khaydukov, Yu.V. Nikitenko, L. Bottyán, A. Rühm, V.L. Aksenov, Crystall. Rep. 55, 1235 (2010).

[4] Yu.N. Khaydukov, V.L. Aksenov, Yu.V. Nikitenko, K.N. Zhernenkov, B. Nagy, A. Teichert, R. Steitz, A. Rühm, L. Bottyán, J. Supercond. Nov. Magn. 24 (2011) 961.

[5] M. Yu. Kharitonov, A. F. Volkov and K. B. Efetov, Phys. Rev. B 73, 054511 (2006)
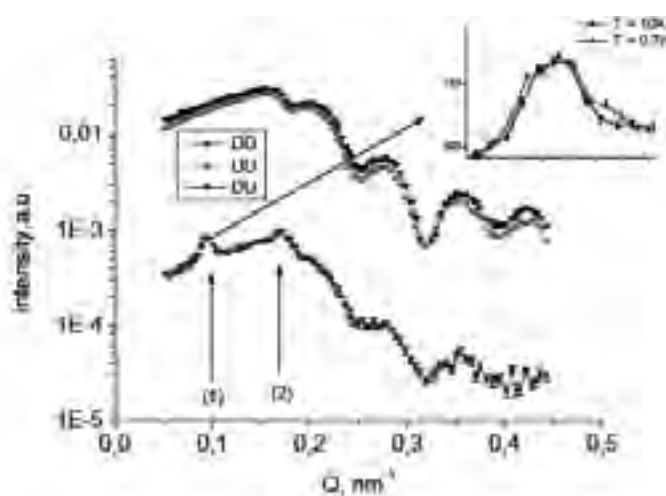
Fig.1: The decrease in the peak width below the superconducting transition temperature of vanadium indicates a change in magnetic structure.

Standardization of low-cross-section nuclides

Z. Révay[1], L. Szentmiklósi[2]

[1]Forschungs-Neutronenquelle Heinz Maier-Leibnitz (FRM II), Garching, Germany
[2]Hungarian Academy of Scienes, Institute of Isotopes, Budapest, Hungary

In-beam prompt activation measurement is the most accurate method for the determination of gamma-ray production cross-sections of nuclides.

If the nuclide has a relatively simple level scheme, a high-accuracy neutron capture cross-sections can also derived. The light stable nuclides (A<20) have low cross-sections for (n,γ) reactions, and also simple level schemes.

The prompt gamma standardization measurements have already been performed in the medium-flux beam at Budapest, but the accuracies were sometimes rather low due to the low cross-section. The PGAA facility of FRM II provides a unique opportunity to measure these materials with a high count rate and with low uncertainties.

The standardization project for nuclides with low cross-section has started 3 years ago, and will be completed using the newly reconstructed PGAA facility, which also provides unique background conditions for this type of experiment. The first result will be presented at the meeting.

Residual stress evolution through manufacture of sub-scale turbine discs

J. Rolph[1], M. Preuss[1], R. Ramanathan[2], M. C. Hardy[3]

[1]University of Manchester, Materials Science Centre, United Kingdom
[2]ATI Ladish Forging, Cudahy, USA
[3]Rolls-Royce plc, Derby, United Kingdom

In modern gas turbines the drive to increase power output and efficiency has lead to increased compressor discharge and turbine entry temperature, thus higher load and operating temperatures for the materials involved. In the turbine section this material is Nickel superalloy, a material which derives high temperature strength from a finely tuned γ/γ´ microstructure. To achieve an optimal microstructure, the material undergoes a sequence of forging and heat treatment processes during which significant residual stresses are generated. In subsequent manufacture, ageing and machining processes then relax and redistribute the residual stress. For engine manfucturers the residual stress distribution during and following manufacture is of significant importance, since it leads to distortion during machining, and governs in-service material performance. Current process modelling efforts aim to characterise residual stress throughout manufacture; in order to validate said models, it is necessary to determine residual stress experimentally. This has been carried out here using neutron diffraction, chosen specifically for this study since it allows characterisation throughout the bulk. Three sub-scale disc forgings of Nickel Superally RR1000 were provided by ATI Ladish Forging each having been designed to represent a stage of the manufacturing process; quench, ageing heat treatment, and material removal through machining.

The sample geometry is shown in Figure 1b. Residual strain measurements were made in the three principal strain directions using using a single diffraction plane Ni(311) with a 4mm^3 spatial resolution on the dedicated strain scanning instrument STRESS-SPEC. A sub-set of the results obtained have been compared to those generated through finite element modelling in Fig.1a.

Residual stress generated through water quenching has been found to reach 1200MPa; in tension in the bore and compression in the rim. Ageing heat treatment relaxed the residual stress by up to 600MPa, but this was reduced where the initial residual stress was lower. Material removal further reduced residual stress by up to 200MPa, the greatest effect being observed in proximity to the machining operation. Agreement between finite element modelling and neutron diffraction data was found to be very strong most measurement locations and conditions.
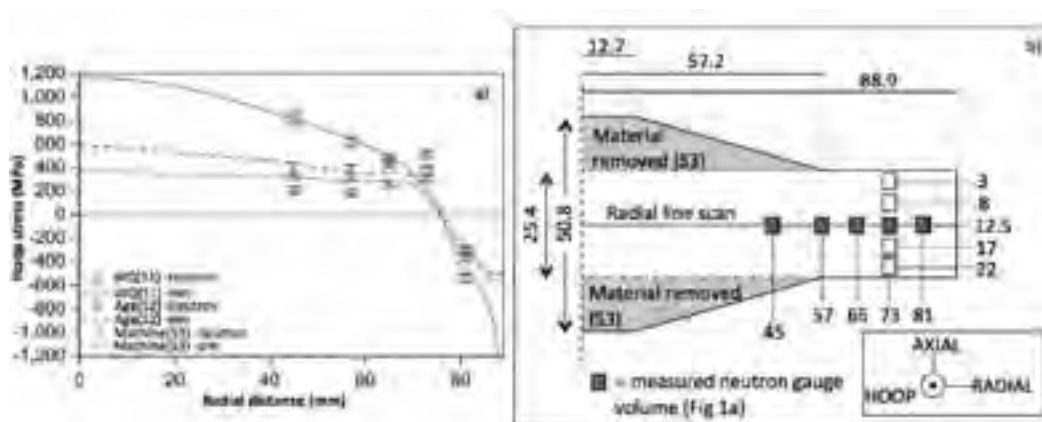
Fig.1:
a) Residual stress line scans through manufacture in the hoop direction.
b) Sample geometry with radial measurement line scan, and measured gauge volumes indicated

A table had been left out by editors due to the lack of space.

Stability and evolution of phases in Co-Re-base alloys during high-temperature exposure

P. Strunz[1], R. Gilles[2], D. Mukherji[3], M. Hofmann[2], M. Hölzel[4], J. Rösler[3]

[1]Nuclear Physics Institute ASCR, Rež near Prague, Czech Republic

[2]Forschungs-Neutronenquelle Heinz Maier-Leibnitz (FRM II), Garching, Germany,

[3]TU Braunschweig, Institut für Werkstoffe, Germany,

[4]TU Darmstadt, Materialwissenschaft, Germany

In the development of new high-temperature alloys for gas turbine applications, various candidates are under consideration. CoRe based alloys [1] strengthened by carbides, eventually by Cr_2Re_3 type σ phase is one promising option. However, the high temperature microstructure and its stability is of great importance for the application. High-temperature cycling experiments performed in-situ on CoRe-1 alloy in parallel with neutron diffraction measurements (Stress-Spec and SPODI) indicate, how heating, cooling and hcp<->fcc phase transformation [2, 3] of the Co-matrix influence the stability of the minority phases during repeated thermal cycles [4].

Neutron diffraction experiments with high-temperature vacuum furnace show that the hysteresis exhibited by $Cr_{23}C_6$ carbides (Fig. 1a) in the second cycle is almost identical to one observed in the first cycle and also follows the hysteresis of Co-hcp phase. On heating, the Cr-carbides start to dissolve at around 1120°C and they are completely dissolved above 1250°C. During cooling, the precipitation of carbides starts approximately at 1150°C. Then, the volume fraction reaches the original value. On the other hand, the σ phase evolution is significantly different in the first and in the second cycle (Fig.1b). s-phase amount increases after the first cycle but it returns to the same value after the second cycle. The second thermal cycle performed on CoRe-1 alloys brought first information on the high-temperature structure and thus on the basic stability during thermal cycling. Further, the influence of boron addition to CoRe-1 (alloy denoted CoRe-1B) was studied for samples undergoing heating/cooling cycle. The diffraction data showed that the basic evolution of phase volume fractions is the same as for the alloy CoRe-1 without boron. A newly developed tensile rig was also tested up to 980°C for the first time at Stress-Spec to combine in-situ loading and heating during neutron diffraction measurements.

[1] J. Rösler, D. Mukherji, T. Baranski: Adv. Eng. Mater. 9 (2007) 876-881

[2] D. Mukherji, P. Strunz, R. Gilles, M. Hofmann, F. Schmitz, J. Rösler: Materials Letters 64 (2010) 2608-2611

[3] D. Mukherji, P. Strunz, S. Piegert, R. Gilles, M. Hofmann, M. Hölzel, J. Rösler: Metall. Mater. Trans. A, (2012) in print

[4] R. Gilles, P. Strunz, D. Mukherji, M. Hofmann, M. Hoelzel and J. Roesler: Journal of Physics: Conference Series, accepted
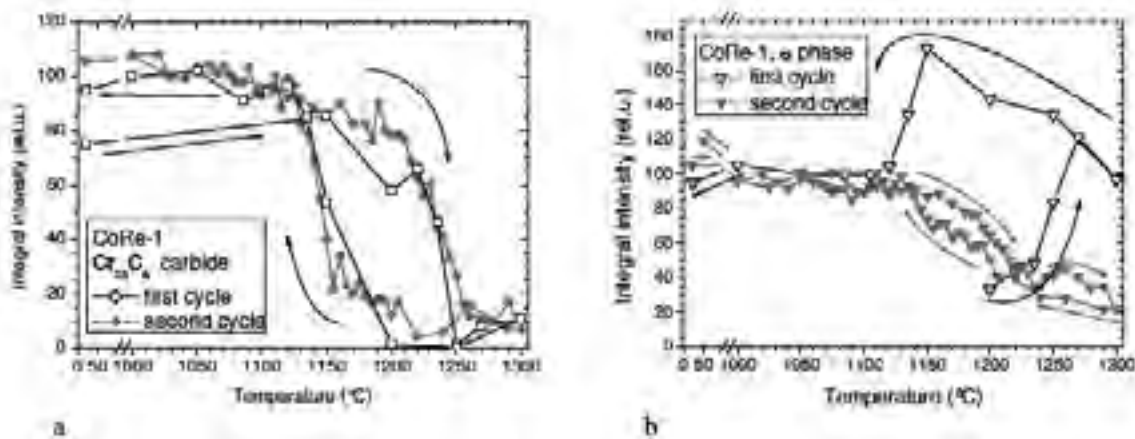
Fig. 1: Evolution of (a) $Cr_{23}C_6$, and (b) σ phase in CoRe-1 during two thermal cycles.

Posters

Magnetic nanoparticles embedded in thin block copolymer

Y. Yao[1], E. Metwalli[1], J.-F. Moulin[2], P. Müller-Buschbaum[1]

[1]TUM, Physik Department, Garching, Germany
[2]Helmholtz-Zentrum Geesthacht, Outstation at FRM II, Garching, Germany

Block copolymers with embedded magnetic nanoparticles have attracted strong interest as a method to fabricate hybrid nanocomposites for wide potential applications in functional nanodevices. Furthermore, the control over the alignment of the nanoparticles within the polymer matrix is essential for producing highly-oriented metal-polymer nanopatterns [1-3]. The control of the alignments and the size of the magnetic nanoparticles arrays can be achieved using a guiding polymer matrix. In this work, we have investigated the alignment of Maghemite nanoparticles within polystyrene (deuterated)-block-polybuthyl methacrylate thin lamellar diblock copolymer films. Metal-polymer hybrid films are prepared by spin coating method. After the heat-annealing step, the metal-polymer hybrid films show a perpendicular lamellar structure (Fig. 1a). It was found that the PS-grafted nanoparticles are selectively adsorbed into one domain of the periodic lamellar structure. We have studied the emerged morphologies under the influence of nanoparticle concentrations using TOF-GISANS. It is obvious that the nanoparticles are swelled into one polymer domain and a distortion of the lamella structure is evolved with increasing of the nanoparticle concentrations.

The total number of TOF channels collected at REFSANS was about 19. In Fig.1c, the solid vertical lines represent the specular peak position while the dotted line represents the material characteristic Yoneda peak. As the wavelength increases the scattering is more surface sensitive and information regarding the metal depth in the polymer film can be gained. Also the ability of the TOF-GISANS to simultaneously measure over a wide range of momentum transfers in one single experiment would allow probing wide range of different nanosized structural features of the sample surface.

[1] E. Metwalli et al., Langmuir 25, 11815 (2009)
[2] V. Lauter-Pasyuk et al., Langmuir 19, 7783 (2003)
[3] E. Metwalli et al. J. Appl. Cryst. 44, 84 (2011)
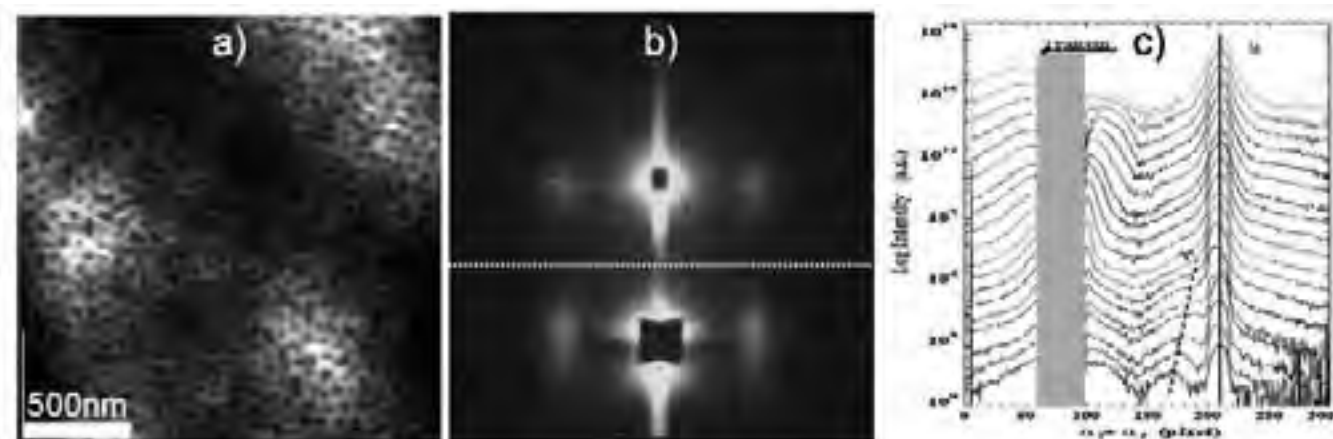
Fig.1. a) AFM images of metal-polymer hybrid film, b) A typical 2d GISANS scattering image of the hybrid film, measured at REFSANS- FRM II. In the 2D pattern the line separate the upper part that represents the reflected signal including the Yoneda peak, the specular peak, and the hybrid film characteristic side peaks, while the lower half of the image contains the transmitted signal. c) The logarithmic intensity as a function of the detector angle for the hybrid film.

Crystallinity-vesicularity interrelation in silicic pyroclasts:
Neutron and X-ray Computed Tomography constraints on magma permeability

S. Wiesmaier[1], B. Scheu[1], K.-U. Hess[1], B. Schillinger[2], A. Flaws[1], D. B. Dingwell[1]

[1]LMU, Earth and Environmental Sciences, München, Germany
[2]Forschungs-Neutronenquelle Heinz Maier-Leibnitz (FRM II), Garching, Germany

The permeability of magma controls gas escape during magma ascent and thus may control eruption behaviour, varying from quiet degassing to explosive fragmentation (Mueller et al., 2008). Yet, the spatial distribution of connected vs. isolated vesicle structures in magma remains poorly constrained. Additionally, the crystal distribution may influence magma permeability: a) do fractures in crystals provide additional pathways to melt-based volatile migration? and b) do low surface-tension crystal faces catalyse bubble nucleation and growth?

In felsic pyroclasts, the size, shape and interconnectivity of vesicles and phenocrysts have been quantified by 3D tomography. We applied high resolution neutron computed tomography (NCT) at 20 μm and X-ray Computed Tomography (XCT) at 5–10 μm resolution on large samples of 15–50 cm^3 to investigate the 3D structure of vesicular (Φ = 0.45–0.72), silica-rich pyroclastic material from various explosive eruptions.

Samples are of the 2004 vulcanian and the 1783 plinian eruption of Asama (Japan), the 1997 eruption of Soufrière Hills Volcano (Montserrat) and the June 1991 vulcanian event of Unzen (Japan).

Volume reconstructions of the pore space and different crystal phases were calculated with Tomoview, our custom-made software. The reconstructed volumes showed an interrelation between vesicle and crystal distribution. Differential overlapping of crystal and vesicle subvolumes trace the crystal outlines exceptionally well. Furthermore, Tomoview detected connected pathways that frequently exploited inter-fracture space of fragmented crystals. Crystal fragmentation thus appears to provide an additional mechanism for generating pore space. The evolution of a permeable network may thus be affected by the crystal content, which ultimately biases the eruptive behaviour of silicic magma.

Nitrogen analysis at orange coloured zinc oxide samples using PGAA

S. Söllradl[1,2], M. Greiwe[3], V. J. Bukas[3], T. Nilges[3], A. Senyshyn[2], L. Canella[2], P. Kudejova[2], A. Türler[1], R. Niewa[4]

[1]Universität Bern and PSI, Villingen, Switzerland

[2]Forschungs-Neutronenquelle Heinz Maier Leibnitz (FRM II), Garching, Germany

[3]TUM, Physik Department, Garching, Germany

[4]Universität Stuttgart, Institut für anorganische Chemie, Germany

Pure Zinc Oxide is a direct, wide band gap semiconductor with a band gap of about 3.4 eV [2]. Pure large crystals are transparent in the visible part of the spectrum. As fine powder it has normally a white colour. Based on a publication in 2009 [1] samples for detection limit measurements of Nitrogen in a ZnO matrix were prepared for prompt gamma activation analysis (PGAA) measurements at FRM II in Munich. More Information about the technique of PGAA can be found in [3-5].

The synthesis was performed as described in [1]. The sample is analysed with Raman spectroscopy, powder x-ray diffraction (PXRD) and PGAA and the results were compared with the results described in literature [1]. During experiments with different ratios of Urea:$Zn(NO_3)_2 \bullet 6H_2O$ an additional phase was detected at a molar ratio of 2.3:1. The product has a pale orange colour. It shows the 4 Raman bands which were discussed in [1] to indicate the presence of nitrogen at 277, 509, 580 an 604 cm^{-1}. Two additional bands were detected at 751 and 1046 cm^{-1}. The PXRD measurements showed additional refelrexions (Fig 1).

The phase is under further investigation. PGAA measurements were performed with the pale orange sample with a molar ratio of Urea:$Zn(NO_3) \bullet 6H_2O$ 2.3:1. In addition to Zn, also H,C,N were detected. Oxygen cannot be measured with PGAA in such a matrix due to the low neutron capture cross section. During tests about the solubility, a white crystalline substance could be separated. Subsequently, the orange powder containing ZnO and the additional phase was dissolved in HCl (conc. 20%) at 70°C. Upon cooling at about 65°C white crystals formed on the surface of the acid. Qualitative EDX (energy dispersive x-ray spectroscopy) measurements showed no occurrence of Zn or Cl within the substance. Only H,C,N,O were detected in EDX. Table 1 compares the results of the PGAA measurement of the 2.3:1 ratio, orange coloured ZnO powder containing the additional phase with an HCN elemental analysis measurement of the white crystals. Due to the low neutron capture cross section of C, the relative error is much larger than of the other elements.

PGAA and HCN elemental analysis show a similar relative abundance of the elements H,C,N. PGAA was able to measure these elements within the ZnO. It is expected that an additional organic phase forms, which resists the harsh conditions during the flame synthesis. The properties of the additional phase are not completely resolved yet.

[1] M. Mapa and C. S. Gopinath, 21, 351–359 (2009).
[2] C. Klingshirn, ChemPhysChem (2007)
[3] G. L. Molnár, Handbook of Prompt Gamma Activation Analysis with Neutron Beams (Kluwer Academic Publishers, 2004)
[4] P. Kudejova, T. Materna, J. Jolie, and G. Pascovici, XRay Spectrom. 34, 350–354 (2005)
[5] M. Crittin, J. Kern, and J. L. Schenker, Nucl. Instrum. Methods Phys. Res., A 449, 221–236 (2000)
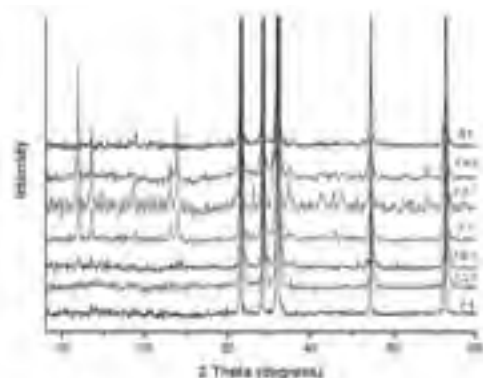
Fig.1: Increase of an additional phase with a maximum intensity at a preparation ratio of 2.3:1. [Cu Kα$_1$, λ=1,5405Å]

Elements	HCN of crystals	PGAA of orange ZnO
H	32.5 ± 0,6%	16 ± 5%
C	32.3 ± 0,6%	23 ± 25%
N	35.1 ± 0,6%	16 ± 6%
Zn	not measured	44 ± 5%

Tab.1: Comparison of the PGAA measurements of orange coloured ZnO (molar ratio 2.3:1) with the separated white crystals separated from HCl (HCN analysis) in %

Solvent distribution in block copolymer thin films

A. Sepe[1], E. T. Hoppe[1], D. Posselt[2], J.-F. Moulin[3], D.-M. Smilgies[4], C. M. Papadakis[1]

[1]TUM, Physik Department, Garching, Germany
[2] Roskilde University, Department of Science, Systems and Models, Denmark
[3]Helmholtz-Zentrum Geesthacht, Outstation at FRM II, Garching, Germany
[4] Cornell University, Cornell High-Energy Synchrotron Source (CHESS), Ithaca, NY, USA

Block copolymer thin films form nanostructures by self-assembly and find a number of applications, especially as templates for structuring inorganic materials, which may be used as data storage devices [1]. However, the usual preparation methods often result in defects which hamper the application. Solvent vapor treatment is frequently used to anneal such defects [2,3].

The aim of the project is to determine the distribution of solvents in lamellar poly(styrene-bbutadiene) (P(S-b-B)) thin films in dependence on the selectivity of the solvent towards PS and PB. Time-of-flight neutron reflectometry (TOF-NR) at the instrument REFSANS together with the use of deuterated solvents may enables us to determine the asymmetry of the lamellae upon swelling and thus the distribution of the solvent [4].

We investigated fully protonated, lamellar P(Sb- B) diblock copolymer (28 kg/mol, film thickness D_{film} = 5000 Å) and fully deuterated cyclohexane (CHX-d_{12}) as a solvent, which is slightly selective to the PB block. At REFSANS at FRM II, NR curves in a q_z-range of 0-0.12 Å^{-1} were measured at four incident angles between 0.22° and 1.14°. A custom-made vapor cell connected to a solvent bubbler was used to swell the film with CHX-d_{12} vapor. The film thickness and the overall degree of swelling were determined in-situ using a VIS interferometer. The TOF-NR curve of the as-prepared film (Fig. 1, lower curve) shows a first-order Bragg reflection at q_z = 0.035 Å^{-1}, thus evidence of parallel lamellar structures with a layer spacing of 180 Å. No second-order Bragg reflection is observed, in accordance with the system having symmetric lamellae where the PS and the PB parts have the same thickness. The TOF-NR curve of the film swollen by CHX-d_{12} (upper curve in Fig.1) shows, instead, a very pronounced Bragg reflection at 0.028 Å^{-1}; this shift reflects the lamellar swelling which amounts to 24%. Higher-order Bragg reflections are observed as well.

To our knowledge, the partitioning of solvent in the block copolymer mesophase has previously been addressed only theoretically [5]. In-situ TOF-NR experiments together with the use of deuterated solvents give detailed insight into the structural changes of the block copolymer thin film during swelling which are not accessible with other methods.

[1] Hamley, I.W. Progr. Polym. Sci. 34, 1161 (2009)
[2] Kim, S.H.; Russell, T.P. et al. Adv. Mater. 16, 226 (2004)
[3] Papadakis, C.M.; Di, Z.; Posselt, D.; Smilgies, D.-M. Langmuir 24, 13815 (2008)
[4] Sepe, A.; Hoppe, E.T.; Posselt, D.; Moulin, J.-F.; Smilgies, D.-M.; Papadakis, C.M. FRM II scientific highlight, 93 (2011)
[5] Lodge, T.P.; Hamersky, M.W.; Hanley, K.J.; Huang, C.I. Macromolecules 30, 6139 (1997)
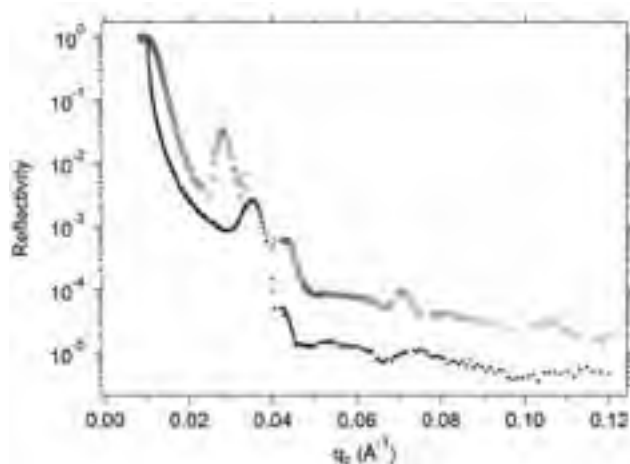
Fig.1: TOF-NR curves of the as prepared (lower curve) and the swollen P(S-b-B) thin film (upper curve).

In-operando neutron scattering studies on Li-ion batteries

A. Senyshyn[1], O. Dolotko[2], M. J. Mühlbauer[2], K. Nikolowski[3], F. Scheiba[3], H. Ehrenberg[2,3,4]

[1]Forschungs-Neutronenquelle Heinz-Maier Leibnitz (FRM II), Garching, Germany

[2]TU Darmstadt, Material Science, Germany

[3]Karlsruhe Institute of Technology (KIT), Institute for Applied Materials (IAM), Eggenstein-Leopoldshafen, Germany

[4]Helmholtz-Institute Ulm for Electrochemical Energy Storage (HIU), Karlsruhe, Germany

Due to the rapid progress in the field of portable electronic and electric vehicles there is an increasing demand for smaller size, larger capacity, lighter weight and lower priced rechargeable batteries. Nowadays the Li-ion batteries are considered as the predominant battery technology due to their high voltage, high energy, good cycle life and excellent storage characteristics. However, despite their overall advantages, Li-ion cells have numerous drawbacks, which can not be overcome and require systematic and detailed research, e.g. on issues concerning safety, price, stability of electrode materials, capacity optimization and cell integration.

Among various approaches towards further battery development, the characterization of the entire battery system during electrochemical cycling seems to be the most promising one as it gives unique information about processes occurring live inside the battery. Such type of "in operando" experiment performed on a real industrial cell should be non-destructive, where all battery constituents remain under real operation conditions and any risks of materials oxidation, electrolyte evaporation or battery charge change are eliminated. In this sense neutron scattering due to its unique features is the excellent tool often having no alternative, when characterization of complex Li-containing systems is under discussion [1]. Thus, the high penetration depths of thermal neutrons suits perfectly for non-destructive studies; the capability to localize light elements/isotopes (e.g. hydrogen, lithium) provides excellent phase contrast; the neutron scattering lengths not dependent on $\sin(\theta)/\lambda$ give accurate structure factors leading to precise bond-length and Debye-Waller factor analysis along with exact determination of lithium diffusion pathways.

The current contribution primarily concerns effects of fatigue processes in lithium ion batteries (which are of primary importance for the battery development purpose) on the evolution of battery constituents on the nano- and micrometer scales. For this purpose a batch of commercial 18650-type Li-ion batteries has been exposed to extensive cycling under controlled temperatures (25C and 50C), which resulted in their prominent fatigue. Its experimental evidences have been obtained by high-resolution neutron powder diffraction studies at diffractometer SPODI [2] performed at different charge/discharge stages. Effects of fatigue on the crystal structure, phase composition, Li-intercalation processes, bond length and microstructure of both cathode and anode electrode materials will be presented along with some correlations to electrochemical properties.

[1] A. Senyshyn, M.J. Mühlbauer, K. Nikolowski, T. Pirling, H. Ehrenberg, "In-operando" neutron scattering studies on Li-ion batteries, J. Power Sources 203 (2012) 126-129

[2] M. Hoelzel, A. Senyshyn, N. Juenke, H. Boysen, W. Schmahl, H. Fuess, High-resolution neutron powder diffractometer SPODI at research reactor FRM II, Nucl. Instr. Meth. A 667 (2012) 32-37

Boron concentration measurements in small organic samples using the PGAA facility at the FRM II

T. Schmitz[1], P. Kudejova[2], C. Schütz[1], J.V. Kratz[1], P. Langguth[3], G. Otto[4], G. Hampel[1]

[1] Universität Mainz, Institute for Nuclear Chemistry, Germany

[2] Forschungs-Neutronenquelle Heinz Maier-Leibnitz (FRM II), Garching, Germany

[3] Universität Mainz, Department of Pharmacy and Toxicology, Germany

[4] Universität Mainz, Department of Hepatobiliary, Germany

Organic specimen, obtained from patients in clinical trials or from in vivo experiments, are usually limited to weights below 100 mg. In a project at the University of Mainz boron concentrations below 30 ppm have to be determined in such small samples. Tissue samples have been measured at the Prompt Gamma Activation Analysis facility at FRM II and the concentration of boron was determined. For the interpretation of the results the obtained peak-area has been determined by an internal standard method while a deconvolution of overlaying peaks with the boron peak was necessary. The determined concentrations are in good agreement with the results of other techniques.

At the University of Mainz the possibilities of Boron Neutron Capture Therapy (BNCT) are investigated in basic research projects in various medical topics. As the name suggests BNCT is based on the neutron capture of the boron isotope 10-B and the following disintegration of the nucleus into an alpha particle and a lithium ion. The basic concept of the therapy is the enrichment of 10-B in tumour cells and their elimination in a following neutron irradiation (Alpha and Li slow down at a path comparable with a cell dimension so the energy of both the particles is able to kill the tumour cells). Today BNCT is applied in phase I and II clinical trials in Finland, Japan and Taiwan mainly to patients with glioblastoma multiforme, head and neck cancer and malignant melanoma.

In 2001 and 2003 also two attempts on the cure of liver cancer using auto-transplantation have been made by a group at the University of Pavia, Italy. Because the liver is surrounded by many radiosensitive organs it needs to be explanted for the irradiation and re-implanted afterwards. Following their experiences it is one aim of the group in Mainz to apply the treatment of liver metastasis in the TRIGA Mark II research reactor of the University of Mainz, which is almost identical in construction than the reactor used in Italy. In an ongoing preclinical trial at the University Hospital Mainz on colorectal carcinoma patients with liver metastases the boron uptake behaviour is investigated. To prevent patients from toxicity effects in a first step only low concentrations of boron are used, which are sufficient for pharmacokinetic studies. Prompt Gamma Activation Analysis has been used successfully in boron detection in a long time. This contribution describes the measurement of small tissue samples using the PGAA facility at the FRM II, which is well established in trace element analysis.

Magnetic anisotropy of the Kondo lattice system CePd$_{1-x}$Rh$_x$

P. Schmakat[1,2,3], M. Schulz[1,2], V. Hutanu[5], M. Brando[3], C. Geibel[3], M. Deppe[3], C. Pfleiderer[1], P. Böni[1]

[1] TUM, Physik-Department, Garching, Germany

[2] Forschungs-Neutronenquelle Heinz Maier-Leibnitz (FRM II), Garching, Germany

[3] ESS Design Update Programme

[4] Max-Planck-Institut für Chemische Physik fester Stoffe, Dresden, Germany

[5] RWTH Aachen, Institut für Kristallographie, Germany

The Kondo lattice system CePd$_{1-x}$Rh$_x$ undergoes a quantum phase transition as a function of Rh content where ferromagnetism is continuously suppressed. The curvature of the phase boundary $T_C(x)$ changes sign for x=0.60. When lowering the transition temperature by substituting Pd by Rh content, a cluster glass phase emerges in the tail region of the phase diagram. We have investigated a single crystal of CePd$_{1-x}$Rh$_x$ with x=0.40 using a ^{3}He cryostat on the instrument POLI-HEIDI. In this study we have cooled down the sample in zero magnetic field and recorded the polarization matrix for several temperatures below and above TC. We found that the single crystal with x=0.40 shows significant magnetic anisotropy, supporting the Ising-like character predicted through magnetisation measurements. The magnetic anisotropy can be directly visualized using the 3D spin manipulation option of the instrument POLI-HEIDI. To illustrate this, we show nutator scans at different temperatures.

[1] T. Westerkamp et al., "Kondo-Cluster-Glass State near a Ferromagnetic Quantum Phase Transition", Phys. Rev. Lett., Vol. 102, 2009, 206404.

[2] J. G. Sereni et al., "Ferromagnetic quantum criticality in the alloy CePd1−xRhx", Phys. Rev. B, Vol. 75, 2007, 024432

[3] C. Pfleiderer et al., "Search for Electronic Phase Separation at Quantum Phase Transitions", J. Low Temp. Phys., Vol. 161, 2010, p.167-181

Residual solvent in adhesive polymer films

M. Schindler[1], O. Soltwedel[2], P. Müller-Buschbaum[1]

[1]TUM, Physik Department, Garching, Germany
[2]Max-Planck-Institute for Solid State Research, Stuttgart, Germany

Pressure-sensitive adhesives (PSAs) are widely applied for their fast and permanent tack, the low force needed for bonding compared to the energy needed for the release and many other advantages like the nearly residual free removal from the adherent. The versatility of PSAs allows for joining very different classes of materials such as paper, glass, polymers and metal [1]. Pressure sensitive adhesives also play a major role in medicine for the removable attachment of patches and sensors to the human skin [2]. PSAs are typically composed of statistical copolymers consisting of a sticky and a glassy component. The sticky component is responsible for wetting the surface (adhesion) while the glassy component ensures proper cohesion and avoids flow of the polymer. Our polymer of choice is a common statistical copolymer consisting of poly(ethylhexylacrylate) as the sticky component and poly(n-butylacrylate) as the glassy component.

Common ways for the preparation of these polymer films are spincoating or solution casting, where the preparation starts from a polymer dissolved in an organic solvent. The solvent evaporates and therefore the films dry during the casting process and afterwards are considered to consist of polymer only. Perlich et al. [3] however found significant remaining solvent for spincast samples of polystyrene (PS) of up to 15 vol% (Fig.2) using neutron reflectivity (NR) measurements. They observed a shift in the critical edge in those samples which were prepared from deuterated solvent (Fig.1) and used this shift to quantify the solvent still present in the sample.

The amount of remaining solvent in the films affects the chain mobility in the film and therefore severly influences the adhesive performance. Also aging of adhesive joints can be affected by solvent residuals. For these reasons we carried out neutron reflectivity measurements to be able to quantify the residuals. Via spincoating films of different thickness (40nm - 500nm) were prepared from both protonated and deuterated solvent (toluene). Thereby we gain contrast to be more sensitive to solvent uptake and can rule out vertical density fluctuations in the films which would be mistaken as enrichment layers. In contrast to [3] we focus on slight modulations in the higher q_z-range to identify solvent enrichment layers at the interface to the substrate. At the FRM II User Meeting 2012 we will present the results of our reflectivity study on the remaining solvent in pressure sensitive adhesive polymer films. The measurements were carried out at the N-REX reflectometer at FRM II.

[1] P. Müller-Buschbaum, T. Ittner, E. Maurer, V. Körstgens and W. Petry, Macromol. Mat. Eng. 292, 793 (2007)
[2] R. A. Chivers, Int. J. Adhes. Adhes. 21:5, 381-388 (2001)
[3] J. Perlich, V. Körstgens, E. Metwalli, L. Schulz, R. Georgii and P. Müller-Buschbaum, Macromol. 42, 337-344 (2009)
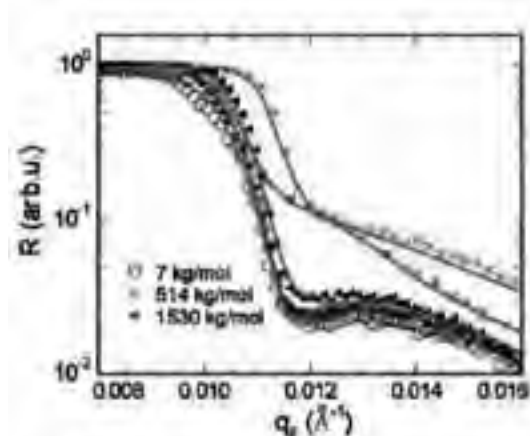
Fig.1: High resolution NR measurements in the region of the critical edge. A shift of the edge due to increased solvent content is clearly visible, taken from [3].
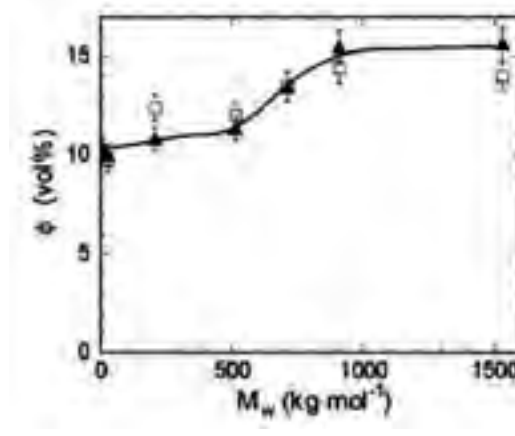
Fig.2: Amount of solvent remaining inside the PS films of different molecular weight M_ω, taken from [3].

Oligomeric state of a membrane protein in a protein-detergent complex studied by contrast variation SANS

F. Zhang[1], A. Pramanik[2], V. Braun[2], F. Roosen-Runge[1], H. Frielinghaus[3], P.Callow[4], F. Schreiber[1]

[1] Universität Tübingen, Institut für Angewandte Physik, Germany
[2] Max-Planck-Institute for Developmental Biology, Tübingen, Germany
[3] Jülich Centre for Neutron Science, Garching, Germany
[4] Institut Laue-Langevin, Grenoble, France

We have studied the oligomerisation of a membrane protein in detergent using small-angle neutron scattering (SANS) via the contrast matching technique [1]. Both the detergent decyl maltoside (DM) and the membrane protein oligomer (ExbB) have been measured by SANS at different contrasts by tuning the composition of the solvent (H_2O/D_2O mixture), i.e. the volume fraction of D_2O. The results show that ExbB-DM forms a globular complex with R_g of 43±0.5 Å, in good agreement with the previous SAXS measurement [2]. The solvent matching point for DM (22.0±1.0% D_2O) is in good agreement to the value reported in the literature and the matching point for ExbB-DM complex is determined to be 29.0±1.0% D_2O volume fraction. Based on the scattering length density of DM, ExbB and the solvent and assuming no D-H exchange in ExbB at the matching point, the mass fraction of DM is obtained as ~0.48. The number of monomers in the protein oligomer has been calculated as 6, i.e. ExbB forms a hexamer in its native state. This is consistent with our previous studies using anthrone calorimetric method [2] and mass spectroscopy [3].

[1] F. Zhang et al., in preparation (2012)
[2] Pramanik, A.; Zhang, F.; Schwarz, H.; Schreiber, F. & Braun, V., Biochemistry, 49 (2010) 8721-8728
[3] Pramanik, A.; Hauf, W.; Hoffmann, J.; Cernescu, M.; Brutschy, B.; & Braun, V., Biochemistry, 50 (2011) 8950-8956.

Investigation of aluminum castings by neutron diffraction

M. Reihle[1]

[1]TUM, Institut für Umformechnik und Gießereiwesen, Garching, Germany

Residual stresses occur in most castings as a result of temperature changes or differences and may reduce fatigue strength and may lead to distortion. Therefore heat treatment is a common method to reduce these mostly unwanted stresses. Especially composite castings, e.g. a cast component consisting of two materials with different thermal expansion coefficients, exhibit significant residual stresses. Existing casting simulations fail in predicting resulting residual strains or stresses accurately. A composite part consisting of a steel insert and a cast aluminum surrounding was investigated. In a first in-situ measurement during the casting process of this composite part large deviations in the strain development during cooling down within the steel insert were detected compared to simulation results (Fig.1). In order to improve residual stress simulation by considering stress relaxation effects, further in-situ measurements will be carried out. Another point of interest is to investigate the effects of heat treatments in Al-Si-Cu alloys with different parameters (temperature and time of solution annealing, temperature and time of aging). Diffraction patterns from different heat treated aluminum samples were obtained at the instrument Stress-Spec (Fig.2) in order to detect the relevant phase Al_2Cu, which has a significant influence on the mechanical properties.
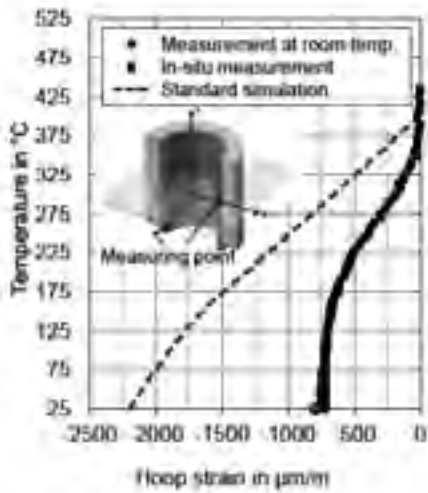
Fig.1: Hoop strain comparison in steel insert of a composite casting (neutron diffraction and elasto-plastic simulation)
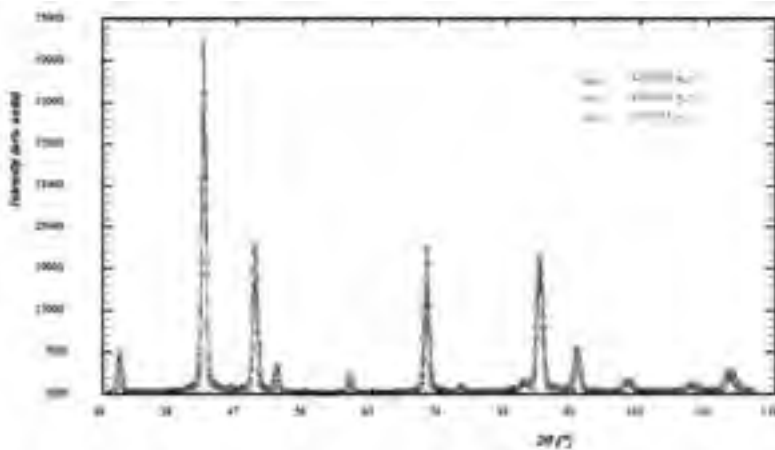
Fig.2: right: picture of sample installation at Stress-Spec; left: exemplary diffraction pattern of three different heat treated samples.

Nanoporous titania-ceramic nanocomposite films for applications in photovoltaics

M. Rawolle[1], K. Sarkar[1], M. A. Niedermeier[1], P. Lellig[2], J. S. Gutmann[2], P. Busch[3], J.-F. Moulin[4], M. Haese-Seiller[4], P. Müller-Buschbaum[1]

[1]TUM, Physik-Department, Garching, Germany

[2]Max-Planck-Institute for Polymer Research, Mainz, Germany

[3]Jülich Centre for Neutron Science, Garching, Germany

[4]Helmholtz-Zentrum Geesthacht, Outstation at FRM II, Garching, Germany

Titania is a widely studied material because of its photoelectric properties. In combination with a ceramic, a hybrid blocking layer with electron percolation paths in the titania can be created, and is applied successfully in solid-state dye-sensitized solar cells (ssDSSCs) [1]. The structure template of a micro-phase separated block copolymer is combined with sol-gel chemistry to create tailored nanostructures. These nanostructures show a higher order and less defects when applying micro-fluidics for the sol-gel templating [2].

With grazing incidence small angle neutron scattering (GISANS) measurements at the JCNS instruments KWS 1 and KWS 2, the inner morphology of the tailored titania-ceramic composite films for different calcination settings is probed. GISANS measurements in the time-of-flight (TOF) mode at the REFSANS instrument (see figure 1) enable to determine the porosity of the titania-ceramic composite films and the degree of backfilling of the titania structures with a hole-conducting polymer, which is of especially high interest for applications in photovoltaics [3].

[1] P. Lellig, M. A. Niedermeier, M. Rawolle, M. Meister, F. Laquai, P. Müller- Buschbaum, J. S. Gutmann, Phys. Chem. Chem. Phys. 14, 1607-1613 (2012)

[2] M. Rawolle, M. A. Ruderer, S. M. Prams, Q. Zhong, D. Magerl, J. Perlich, S. V. Roth, P. Lellig, J. S. Gutmann, P. Müller-Buschbaum, Small 7, 884-891 (2011)

[3] G. Kaune, M. Haese-Seiller, R. Kampmann, J.-F. Moulin, Q. Zhong, P. Müller- Buschbaum, J. Polym. Sci. Part B: Polym. Phys. 48, 1628-1635 (2010)
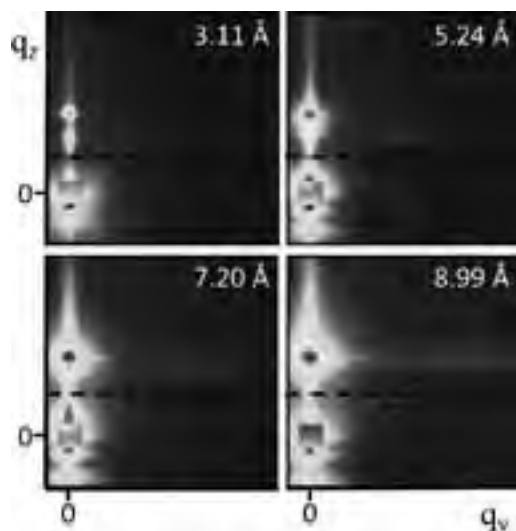
Fig.1: Example of 2d GISANS data of nanoporous titania-ceramic composite film, measured at the beamline REFSANS. The average wavelength is noted in the respective images. The upper half of the 2d patterns contains the reflected signal with the Yoneda peak and the specular peak in q_z-direction and a peak originating from a lateral structure in q_y direction that changes position with the wavelength because of the changing q-range. The lower half contains the transmitted signal where a beamstop at the axes origin blocks the direct beam signal. The dashed lines indicate the sample horizon.

Recent progress in deposition and quantum efficiency measurements of magnetron sputtered B$_4$C-converter layers.

G. Nowak[1], M. Störmer[1], Ch. Horstmann[1], R. Kampmann[1], M. Haese-Seiller[2], J.-F. Moulin[2], D. Höche[1], M. Müller[1], A. Schreyer[1]

[1]Helmholtz-Zentrum Geesthacht, Germany

[2]Helmholtz-Zentrum Geesthacht, Outstation FRM II, Garching, Germany

We report on the recent progress in DC sputter deposition of B$_4$C-layers onto small Si (001) substrates and large Al-detector plate elements at room temperature. The thicknesses of B$_4$C layers were prepared in the range from 0.5 µm up to 2 µm – this is the relevant thickness range for neutron detection used at grazing incidence angles. First results showed that a 1µm thick B^{4}C film possesses high compressive stress and does not adhere directly onto a silicon substrate. A titanium bonding layer between substrate and film allows to coat more than 1 µm thick B$_4$C layer. Furthermore, we investigated the thickness uniformity of the B$_4$C layers over the whole deposition area of 120 mm x 1500 mm using step height measurements by means of a stylus profiler. A slight deviation in B$_4$C film thickness of less than 4% from the arithmetic averages in both in-plane directions was determined (Fig.1 and Fig2). In ongoing investigations we have characterized the chemical depth profile of the sputter deposited B$_4$C films by means of XPS / SIMS.

At the reflectometer REFSANS (FRM-II), the quantum efficiency of the converter samples at different incidence angles were investigated. Very high efficiency (about 50% at α_i= 0.3° nm and more than 80 % for long wavelengths (λ> 0.5 nm)) has been observed at an incidence angle of α_i ~ 0.5°. It is remarkable that the same efficiency is expected for α_i ~ 2.5° if the converter is coated with 1µm thick enriched ^{10}B$_4$C (Fig.3). Incidence angles of 2.5° are currently strived for in our design for detectors in inclined geometry. Thus, the measurements indicate already that very high detection efficiency can be achieved by this detector design.
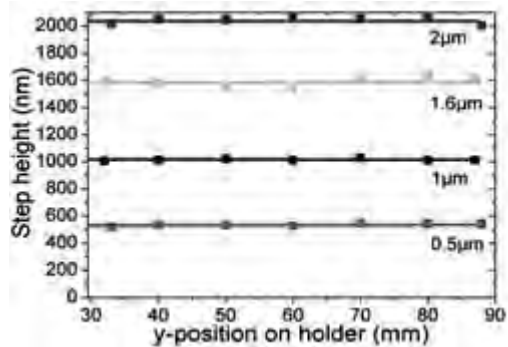
Fig. 1
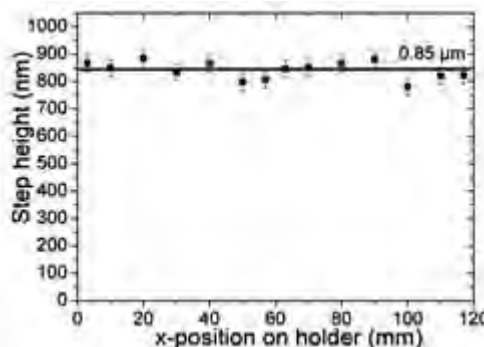
Fig. 2
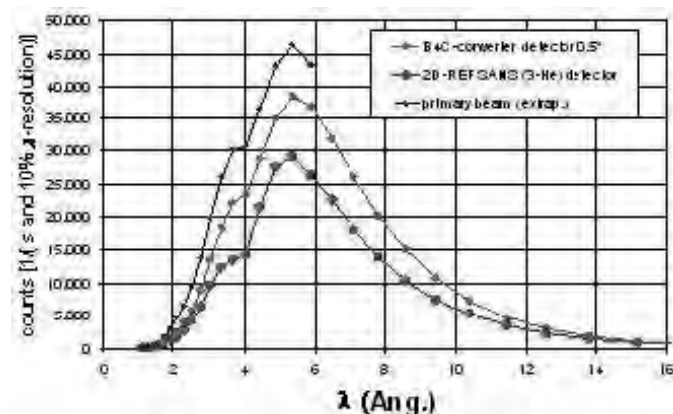
Fig. 3: Comparison between He-3-detector (REFSANS) and B$_4$C-converter detector.

Neutron scattering measurements a useful alloy development tool for the new generation high temperature alloys based Co-Re system

D. Mukherji[1], J. Wehr[1], P. Strunz[2], R. Gilles[3], M. Hofmann[3], M. Hölzel[4], J. Rösler[1]

[1]TU Braunschweig, Institut für Werkstoffe, Braunschweig, Germany,

[2]Nuclear Physics Institute ASCR, Řež near Prague, Czech Republic

[3]TUM, Forschungs-Neutronenquelle Heinz Maier-Leibnitz (FRM II), Garching, Germany,

[4]TU Darmstadt, Materialwissenschaft, Germany

Development of high temperature material is mainly driven by gas turbine needs. Today, Ni-based superalloys are the dominant material class in the hot section of gas turbines, but they are limited by their melting range for applications at ultra-high temperatures needed for the future gas turbines [1]. High melting Co-Re-Cr based alloys introduced by the research group at TU Braunschweig in 2007 [2] show promise as a new material class for such application. The Co-Re alloys have a complex microstructure with many phases present in different morphologies in different length scales [2, 3]. Depending on the alloy composition the phases include Cr- and Ta- carbides and Cr_2Re_3-type σ phase. In the Co-Re-Cr base alloys the Co-solid-solution matrix undergoes an allotropic modification from εCo (hcp) to γCo (fcc) at temperatures above 1200°C [3].

Although Co-base alloys are used in gas turbines at present the Co-Re-Cr system is new for high temperature structural applications and very limited literature is presently available. Neutron scattering has been extensively used in our development work to supplement microstructural investigations and fill in the gap in the literature data. Very useful information is obtained through high temperature in-situ neutron diffraction measurements, which is invaluable for the alloy development. Some selected results will be presented here. Fig.1 shows results from in-situ diffraction measurements at FRM II on a Co-Re based alloy designated CoRe-1 (Co-17Re-23Cr-2.6C). A heating / cooling cycle between 1100° and 1300°C shows the hcp⇆fcc phase transformation of the Co matrix [3,4]. It may be noted that pure cobalt exists in two allotropic forms: low temperature ε (hcp) and high temperature γ(fcc) phases and undergoes fcc⇆hcp allotropic transformation around ~ 420°C - by a diffusionless martensitic mechanism.

[1] J. H. Perepezko, Science, 326 (2009) 1068-1069

[2] J. Rösler, D. Mukherji, T. Baranski: Adv. Eng. Mater. 9 (2007) 876-881

[3] D. Mukherji, P. Strunz, R. Gilles, M. Hofmann, F. Schmitz, J. Rösler: Materials Letters 64 (2010) 2608-2611

[4] D. Mukherji, P. Strunz,, S. Piegert, R. Gilles, M. Hofmann, M. Hölzel, J. Rösler: Metall. Mater. Trans. A, (2012) in print
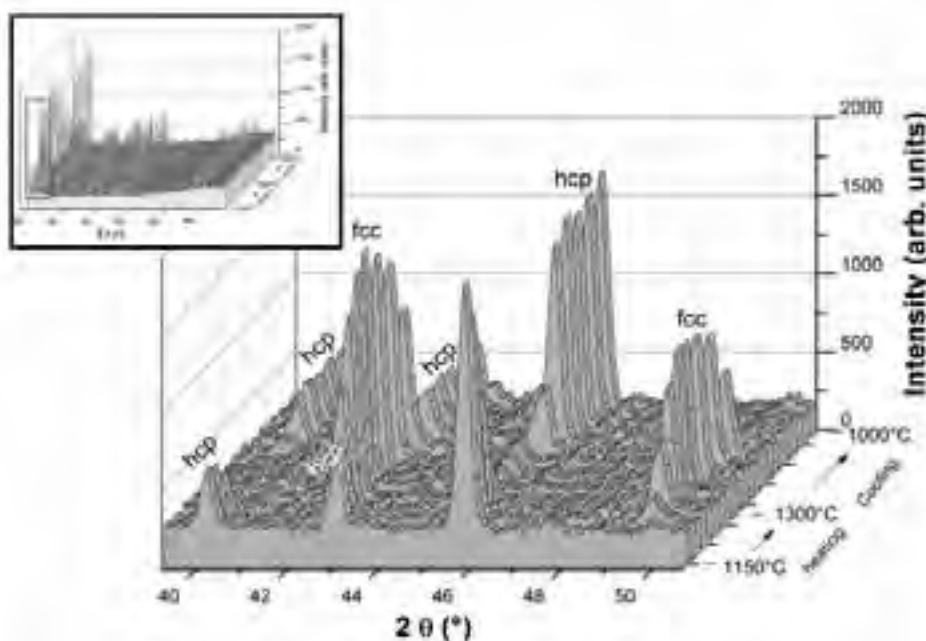
Fig.1: a) Diffractograms measured on CoRe-1 sample during in-situ heating at SPODI. The transformation: hcp→fcc occur on heating and the phase transformation is reversed on cooling. An hysteresis in the hcp⇆fcc transformation was observed for the first time by these neutron diffraction measurements.

Investigation of T-odd effects in fission induced by polarized neutrons

Y. N. Kopatch[1,2], G. V. Danilyan[1], J. Klenke[3], V. A. Krakhotin[1], V. V. Novitsky[1,2], V. S. Pavlov[1], H. Saul[3], P. B. Shatalov[1]

[1]Alikhanov Institute for Theoretical and Experimental Physics, Moscow, Russia
[2]Frank Laboratory of Neutron Physics, JINR, Dubna, Russia
[3]Forschungs-Neutronenquelle Heinz Maier-Leibnitz (FRM II), Garching, Germany

Since many years there have been numerous attempts to find effects which could be the manifestation of the time reversal invariance violation in neutron induced reactions. The experiment performed at the ILL (Grenoble) in 1998, which investigated the three-vector correlation in ternary fission induced by cold polarized neutrons showed unexpectedly large T-odd effect [1]. Although it is believed that the observed effect is not due to the time reversal invariance (TRI) violation, but rather due to the complicated mechanism of the ternary fission process, this effect is commonly called in literature as the TRI-effect. Later, another T-odd effect was discovered in ternary fission, which was named ROT-effect, since it manifested itself as the rotation of the polarized nucleus in the plane perpendicular to the captured neutron spin direction [2].

After the discovery of the T-odd effects in ternary fission at the ILL, a series of experiments were performed by the Russian-German collaboration, first in HMI (Berlin), then at the MEPHISTO instrument of FRM II (TUM, Garching) in order to search for similar effects in angular correlations of prompt gamma-rays and neutrons in binary fission instead of alpha-particles from ternary fission. Since the number of emitted gamma-rays and neutrons in fission is by several orders of magnitude higher than the number of alphaparticles, accompanying fission, the sensitivity of such measurements allowed to achieve the accuracy of the measured effects of about $10^{-5} \div 10^{-6}$. Soon it was clearly and unambiguously demonstrated that the ROT-effect for gamma-rays exists, its sign is the opposite and its size is about one order of magnitude smaller as compared to the effect for the α-particles [3]. In the last experiments at the MEPHISTO of FRM II also the ROT-effect in neutron emission was discovered, having even smaller magnitude [4]. However, no signs of the TRI-effect have been found up to now in neutron or gamma-ray emission.

It's worthwhile to mention that the nature of discovered T-odd effects in the emission of a-particles, gamma-rays and neutrons can be completely different. Several theoretical models already exist, which give qualitative and sometimes also quantitative explanations and predictions for these effects. More experimental efforts are needed in order to verify the theories and understand the nature of these interesting phenomena. The detailed investigation of the T-odd effects in fission is currently under way and planned for the future at the MEPHISTO instrument of the FRM II.

[1] P. Jesinger, G. V. Danilyan, A. M. Gagarski, et al., Phys. Atom. Nucl. 62, 1608 (1999)
[2] F. Goennenwein, M. Mutterer, A. Gagarski, et al., Phys. Lett. B 652, 13 (2007)
[3] G. V. Danilyan, J. Klenke, V. A. Krakhotin, et al., Phys. Atom. Nucl. 72, 1812 (2009)
[4] G. V. Danilyan, J. Klenke, V. A. Krakhotin, et al., Phys. Atom. Nucl. 74, 671 (2011)

Recent progress in the development of gaseous boron converter detector with inclined geometry

R. Kampmann[1,2], G. Nowak[1], M. Störmer[1], Ch. Horstmann[1],T. Kühl[2], E. Prätzel[2], M. Haese-Seiller[1], J.-F. Moulin[1], D. Höche[1], R. Hall-Wilton[3], M. Müller[1], A. Schreyer[1]

[1]Helmholtz-Zentrum Geesthacht, Geesthacht, Germany
[2]DENEX Detektoren für Neutronen GmbH, Lüneburg, Germany
[3]European Spallation Source ABB Detector Group, Lund, Sweden

The recent development of 2D-position-sensitive neutron detectors with thin boron converter layers in inclined geometry currently comprises on the one hand the production of 0.5 µm up to 2 µm thick $^{nat}B_4C$-converter layers by means of DC sputtering on large Al-converter plates. On the other hand a dedicated test detector has been designed and manufactured on the basis of a DENEX-300TN detector to characterize the quantum efficiency as well as the spatial resolution at small (and large) incidence angles of the primary beam onto the converter surface. The ToF-reflectometer REFSANS was used for first experiments.

Al-converter samples with a size of 100 mm × 100mm × 0.5 mm were coated with 1 µm thick $^{nat}B_4C$ and mounted in the test detector (Fig. 1). The detector was pre-characterized with an Am-Be source and a wide plateau of the characteristic curves (count rates versus anode voltage) was found. This indicates high quantum efficiency of the 2D-detector for all ^{7}Li-nuclei and α-particles which escape out of the conversion layer and ionize the detection gas. Afterwards the test detector was mounted on the REFSANS goniometer and the efficiency as well as position resolution was measured in dependence of the incidence angle $α_i$ and the wavelength λ. Very high quantum efficiency was found for $α_i$ = 0.5° (~ 50% for λ =0.3 nm and more than 80 % for λ > 0.5 nm; Fig. 2). If the coating would consist of $^{10}B_4C$ instead of $^{nat}B_4C$ this high quantum efficiency is to be expected for $α_i$ ~ 2.5° due to the fact that the content of ^{10}B is only ~ 20% in ^{nat}B. Incidence angles of $α_i$ ~ 2.5° are strived for in our final detector design. Thus, the measurements already disclose the high quantum efficiency which can be achieved by our detector design. The test detector has a 2D-position readout with a spatial resolution of δd ~ 2 mm. In the inclined geometry the resolution is improved in the direction perpendicular to the converter surface by the factor 1/sin $α_i$. This results in a resolution of δd < 0.1 mm for $α_i$ ~ 0.75°. This high resolution was verified experimentally, e.g. the intensity profile of the 0.5 mm wide REFSANS beam as well its shift by 0.1 mm perpendicular to the converter surface could easily be measured. The detector development is performed as an in-kind contribution to the ESS instrumentation, and is part of the German support to the ESS Pre-Construction Phase and Design Update.

Fig.1: Test detector with mounted samples.
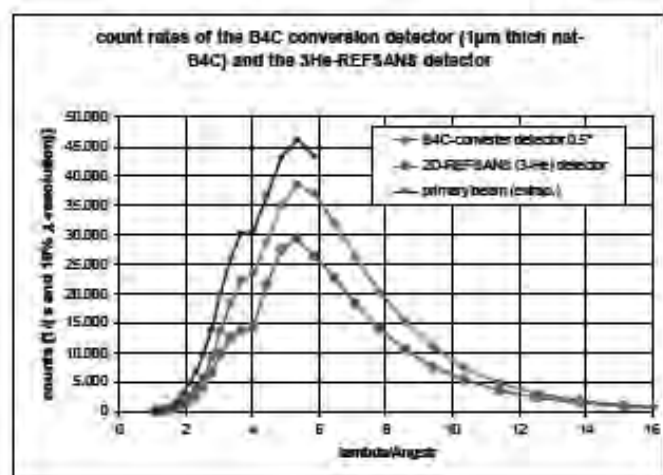
Fig.2: Count rates.

Switching behavior of thermoresponsive poly(2-oxazoline) copolymers in aqueous solution

S. Jaksch[1], J. Adelsberger[1], S. Salzinger[2], S. Huber[2], R. Jordan[2,3], Z. Di[4], C. M. Papadakis[1]

[1]TUM, Physik Department, Garching, Germany

[2]TUM, Department Chemie, Garching, Germany

[3]TU Dresden, Department Chemie, Germany

[4]Jülich Centre for Neutron Science, Garching, Germany

Thermoresponsive polymers in aqueous solution exhibit a strong change in solubility and volume when heated above their cloud point. Poly(2-oxazoline)s (POx) represent a very attractive class of these materials as their properties can be tuned from hydrophobic over thermoresponsive to hydrophobic by a pendant 2-substitution [1,2]. Moreover they are non-toxic and biocompatible which makes them ideal candidates for medical applications [3]. We have studied the aggregation behavior of poly(iso-propyl-2-oxazoline)$_{50}$ (PiPrOx$_{50}$) as a reference homopolymer as well as poly[(iso-propyl-2-oxazoline)-(n-nonyl-2-oxazoline)]$_{grad}$ gradient copolymers (P[iPrOx$_{48}$NOx$_2$]$_{grad}$ and P[iPrOx$_{46}$NOx$_4$]$_{grad}$) around their cloud points [4]. The inclusion of the hydrophobic NOx moieties changes the cloud point from 40.3°C for PiPrOx$_{50}$ to 25.2°C and 23.2°C for P[iPrOx$_{48}$NOx$_2$]$_{grad}$ and P[iPrOx$_{46}$NOx$_4$]$_{grad}$ respectively.

To elucidate the aggregation behavior, we performed temperature dependent small angle neutron scattering (SANS) experiments at KWS 1 at FRM II on aqueous solutions of all polymers (20 mg/ml in D$_2$O). The curves feature both single chain scattering (above q=0.2 nm^{-1}) and forward scattering due to large aggregates, see Fig. 1. The curves were modeled by a superposition of scattering from Gaussian chains and large spheres (PiPrOx$_{50}$ and P[iPrOx$_{48}$NOx$_2$]$_{grad}$) or of small and large spheres (P[iPrOx$_{46}$NOx$_4$]$_{grad}$).

While for the homopolymer, aggregation to large aggregates sets in immediately upon heating above the cloud point, the gradient copolymers form precursor aggregates of a few chains already below the cloud point, see Fig. 2. These remain stable up to 5 K above the cloud point and merge into large aggregates at higher temperatures. Thus an intermediate regime is observed. We attribute these precursor aggregates to the additional NOx moieties forming bridges between the dissolved chains which remain stable even above the cloud point. We thus conclude that the aggregation of the gradient copolymers is a two-step process with an onset of aggregation already below the macroscopic cloud point. The small aggregates are stable even above the cloud point, and only at more elevated temperatures, large aggregates are favored.

[1] T.B. Bonné, K.Lüdtke, R. Jordan, C.M. Papadakis, Macromol. Chem. Phys. 208, 1402-1408 (2007)

[2] R. Ivanova, T. Komenda, T.B. Bonné, K. Lüdtke, K. Mortensen, P.K. Pranzas, R. Jordan, C.M. Papadakis, Macromol. Chem. Phys. 209, 2248-2258 (2008)

[3] F.C. Gärtner, R. Luxenhofer, B. Blechert, R. Jordan, M. Essler, J. Contr. Release 119, 291-300 (2007) [4] S. Salzinger, S.Huber, S. Jaksch, R. Jordan, C.M. Papadakis, Coll. Polym. Sci. DOI:10.1007/s00396-011-2564-z

Fig.1: Representative scattering curves for PiPrOx50. Solid lines are fits.
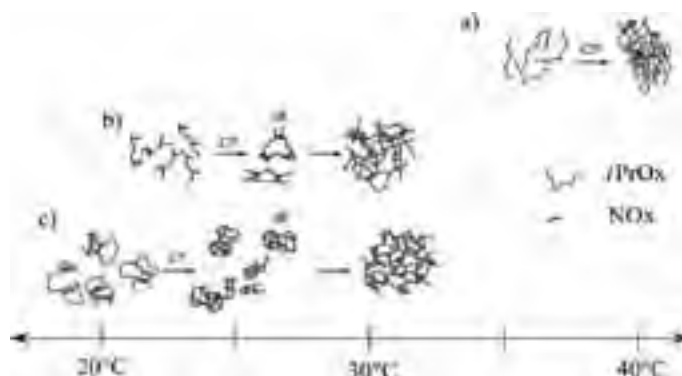
Fig.2: Sketch of the aggregation behavior of PiPrOx50 (a)), P[iPrOx$_{48}$NOx$_2$]$_{grad}$ and P[iPrOx$_{46}$NOx$_4$]$_{grad}$ (b) and c)).

Neutron induced activation of $LaBr_3$:Ce and $CeBr_3$ scintillating crystals

A. Iyudin[1,2] , V. Bogomolov[1,2], T. Bücherl[3], A. von Kienlin[4] , S. Svertilov[1,2]

[1]Skobeltsyn Institute of Physics, Moscow, Russia

[2]Lomonosov Moscow State University, Russia

[3]Radiochemie München, Garching, Germany

[4]Max-Planck-Institut für Extraterrestrische Physik, Garching, Germany

Recent advances in scintillating materials development have resulted in the availability of $LaBr_3$:Ce and $CeBr_3$ crystals combining fast light decay with high light yield and stopping power. The detectors based on these crystals have energy resolution <3% (for ~1MeV energy deposition) and sub-nanosecond time resolution. The main factor limiting the use of $LaBr_3$:Ce is its internal background coming from naturally occurring isotope ^{138}La and ^{227}Ac pollution. $CeBr_3$ crystals have much lower background rate.

$LaBr_3$:Ce and $CeBr_3$ crystals are planned for a use in a future space experiments. In this case a problem of a crystal radiation hardness arises. Considering low orbit experiments a number of factors such as irradiation by galactic and solar cosmic rays, or by protons of inner radiation belt are present. Energetic protons produce also neutrons coming from the Earth atmosphere (albedo neutrons) as well as from the spacecraft itself (local neutrons).

Taking into account the difference in background producing reactions by protons and neutrons as well as the difference between $LaBr_3$:Ce and $CeBr_3$ composition we performed tests of radiation hardness of $LaBr_3$:Ce and $CeBr_3$ scintillating crystals with the use of a neutron beam at the NECTAR facility of FRM II.

In this presentation we compare results of the fast neutron induced activation of $LaBr_3$:Ce with doses 10^9-10^{12} n/cm^2 with that of proton induced activation, as well as an activation due to number of isotopes with half life values from several hours to a hundred days.

Neutron diffraction on functional materials under special environmental conditions

M. Hölzel[1], A. Senyshyn[1], M. Hinterstein[2], W. W. Schmahl[3], F. Dolci[4], H. Fuess[5]

[1]Forschungs-Neutronenquelle Heinz Maier-Leibnitz (FRM II), Garching, Germany

[2] TU Dresden, IFW Dresden, Germany

[3]LMU, Department für Geo- und Umweltwissenschaften, München, Germany

[4]Joint Research Center of the European Commission, Cleaner Energies Unit Petten, The Netherlands

[5]TU Darmstadt, Fachbereich Material- und Geowissenschaften, Germany

This contribution presents neutron diffraction studies on technologically attractive materials with the main focus on the ferroelectric ceramics under high electric fields. The investigations were carried out at the high-resolution neutron powder diffractometer SPODI, which offers possibilities for in-situ materials characterisation under various environmental conditions [1].

Ferroelectric ceramics were investigated under the influence of high electric fields to establish correlations between the macroscopic poling behaviour and corresponding structural changes. The investigations were performed on lanthanum doped lead zirconate titanate (PLZT) with compositions around the morphotropic phase boundary [2] and also on a bismuth sodium titanate based system (BNT-BT-KNN) [3], which stands as a lead-free counterpart of PLZT. A self-designed sample environment allows to apply high electric fields up to 7 kV/mm (35 kV) on bulk samples in a SF6 gas atmosphere at room temperature. Different setups are available with the electric field direction either vertical to the scattering plane or within the scattering plane. In two compositions of the system BNT-BT-KNN a field induced macroscopic strain could be explained by a phase transformation during the poling process. In both cases the transition to a rhombohedral phase was identified by corresponding superlattice reflections, arising from a superstructure in the tilting angles of the oxygen octahedra around Ti/Zr atoms. The phase fractions and structural parameters have been obtained by full-profile Rietveld refinement technique.

In lanthanum doped PZT samples with different Ti/Zr compositions, different types of structural distortions under the influence of electric fields were identified. Systematic changes in the response to the electric field were observed for different compositions across the morphotropic phase boundary.

Some recent and enhanced possibilities of materials characterization at neutron powder diffractometer SPODI will be mentioned in brief: a rotatable tensile rig enabling the determination of the elastic anisotropy in nickel-titanium shape memory alloys; the structural changes in lithium-ion batteries during charging/discharging monitored "in-operando" using a multi-channel potentiostate; a gas pressure cell for deuterium charging at high deuterium pressures (up to 100 bar) as a result of collaboration with the Joint Research Centre of the European Commission [4].

[1] M. Hoelzel, A. Senyshyn, N. Juenke, H. Boysen, W. Schmahl, H. Fuess, Nucl. Instr. Meth. A 667 (2012) 32-37

[2] M. Hinterstein, M. Hoelzel, H. Kungl, M.J. Hoffmann, H. Ehrenberg, H. Fuess, Z. Krist. 226 (2011) 155-162

[3] M. Hinterstein, M. Knapp, M. Hoelzel, W. Jo, A. Cervellino, H. Ehrenberg, H. Fuess, J. Appl. Cryst. 43 (2010) 1314-1321

[4] F. Dolci, E. Weidner, M. Hoelzel, T. Hansen, P. Moretto, C. Pistidda, M. Brunelli, M. Fichtner, W. ohstroh, Int. J. Hydr. Energy 35 (2010) 5448-5453

Hindered rotational energy barriers of BH_4^- tetrahedra in β-Mg($BH_4)^2$ from quasielastic neutron scattering and DFT calculations

D. Blanchard[1], J. B. Maronsson[1,2], M. D. Riktor[3], J. Kehres[1], D. Sveinbjörnsson[1], E. Gil Bardají[4],

A. Léon[4], F. Juranyi[5], J. Wuttke[6], K. Lefmann[7], B. C. Hauback[3], M. Fichtner[4], T. Vegge[1]

[1]Technical University of Denmark, Division of Energy Conversion and Storage, Roskilde, Denmark

[2]Technical University of Denmark, Center for Atomic Scale Materials Design, Lyngby, Denmark

[3]Institute for Energy Technology, Physics Department, Kjeller, Norway

[4]Karlsruhe Institute of Technology (KIT), Institute of Nanotechnology, Germany

[5]Laboratory for Neutron Scattering ETH Zurich and Paul Scherrer Institute Villigen PSI, Switzerland

[6]Jülich Centre for Neutron Science, Garching, Germany

[7]Niels Bohr Institute, Nanoscience Center, København, Denmark

In this work, hindered rotations of the BH_4^- tetrahedra in Mg($BH_4)^2$ were studied by quasielastic neutron scattering, using two instruments with different energy resolution, in combination with density functional theory (DFT) calculations. Two thermally activated re-orientations of the BH4 - units, around the two-fold (C_2) and three-fold (C_3) axes were observed at temperatures from 120 to 440K. The experimentally obtained activation energies (E_{aC2}=39 and 76 meV and E_{aC3}=214 meV) and mean residence times between re-orientational jumps are comparable with the energy barriers obtained from DFT calculations. A linear dependency of the energy barriers for rotations around the C_2 axis parallel to the Mg-Mg axis with the distance between these two axes was revealed by the DFT calculations. At the lowest temperature (120 K) only 15% of the BH_4^- units undergo rotational motion and from comparison with DFT results it is expectedly the BH_4^- units with the boron atom closest to the Mg-Mg axis, although dynamics related to local disorder existing at the boundary of the anti-phase domains or to the presence of solvent in the sample cannot be strictly excluded. No long-range diffusion events were observed.
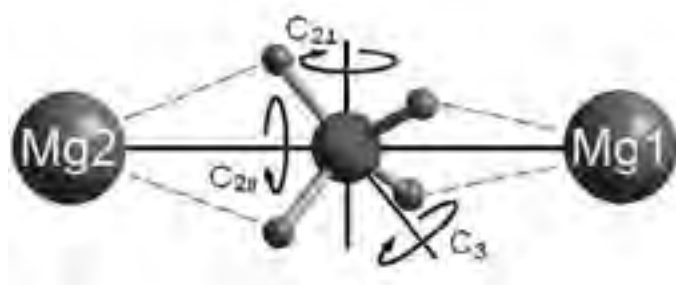
Fig.1: Schematic representation of the coordination environment, with the two-fold $C_{2//}$ and $C_{2\perp}$-axis and a three-fold C_3-axis, of a BH4 unit. From large to small size spheres: Mg, B and H atoms. $C_{2//}$ is the two-fold axis in the direction of the M_{g1}-M_{g2} axis, $C_{2\perp}$ is one of the axis perpendicular to the M_{g1}-M_{g2} axis.
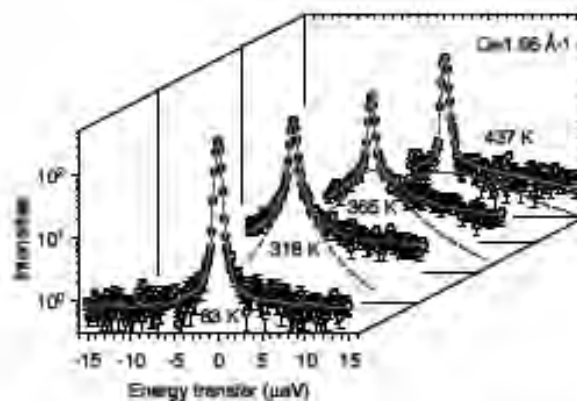
Fig.2: The QENS spectra of ß-Mg($BH_4)_2$ measured with SPHERES at different temperatures for Q =1.66 Å^{-1}. The dots are the experimental data. The solid red lines display the fits of the data, each consisting of a resolution broadened delta function, a Lorentzian (dashed green lines) and a flat background (not shown on the plots).

Wall thickness texture inhomogeneities of a Cu-tube investigated by the Stress-Spec robot

N. Alhamdany[1], W. Gan[2], C. Randau[3], M. Völler[4], H.G. Brokmeier[1], M. Hofmann[4]

[1]TU Clausthal, Institut für Werkstoffkunde und Werkstofftechnik, Germany.

[2]Helmholtz-Zentrum Geesthacht, Outstation at FRM II, Garching, Germany.

[3] Georg-August-Universität, Geowissenschaftliches Zentrum Göttingen, Germany.

[4]Forschungs-Neuttronenquelle Heinz Maier-Leibnitz (FRM II), Garching, Germany.

Texture variations are present in most samples, which are due to materials processing. The production of highly precise tubes has two main manufacturing problems, the anisotropy around the perimeter and the anisotropy over the wall thickness.

Due to the restricted free space inside the Eulerian cradle the sample movement is limited. In order to overcome the spatial limitation for sample manipulation and to be more flexible in texture mapping a robot system based on an industrial Stäubli RX160 robot has been used [1].

A first investigation was performed using a Cu ring of 140 mm diameter, 10 mm wall thickness and 11 mm length cut from a Cu tube. Due to the slit system a gauge volume between 1511 mm³ and 6527 mm³ was used to get the texture variation around half of the perimeter every 15°. With one robot set up we obtain 45° at the perimeter. In a second try a part of the Cu tube was investigated having a weight of about 12 kg with a length of 250 mm. Therefore a special sample holder has to be constructed. It has to be noticed that in both cases the sample must be scanned with laser scanning system to describe the scanning matrix and values for intensity corrections. During pole figure measurement gauge volume is changing due to sample rotation and sample tilt that measured intensities must be corrected for constant volume and anisotropic absorption.

Data analysis was carried out by the software package StressTextureCalculator (STeCa) to extract pole figure data from area detector data [2] using the mathematical formalism of Bunge [3] and by the iterative series expansion method ISEM [4]. Data processing and results will discussed, which show a slight variation of the global texture around the perimeter.

[1] H.-G. Brokmeier, W.M. Gan, C. Randau, M.Völler, J. Rebelo-Kornmeier, M.Hofmann, Nuclear Instruments and Methods in Physic Research A642 (2011) 87-92.
[2] C. Randau, U. Garbe, H.-G. Brokmeier, J. Appl. Crystallogr, 44 (2011) 641-646.
[3] H. J. Bunge, H. Klein: Z. Metallkunde 87(1996) 465-75
[4] M. Dahms, H. J. Bunge J. Appl. Cryst. 22 (1989) 439-447.

Long-range crystalline nature of the skyrmion lattice in MnSi

<u>T. Adams</u>[1], S. Mühlbauer[2], C. Pfleiderer[1], F. Jonietz[1], A. Bauer[1], A. Neubauer[1], R. Georgii[2], P. Böni[1], U. Keiderling[3], K. Everschor[5], M. Garst[5], A. Rosch[5]

[1]TUM, Physik Department, Garching, Germany

[2]Forschungs-Neutronenquelle Heinz Maier-Leibnitz (FRM II), Garching, Germany

[3]ETH Zürich , Institut für Festkörperphysik, Switzerland

[4]Helmholtz-Zentrum Berlin, Germany

[5]Universität zu Köln, Institute of Theoretical Physics, Germany

We report small angle neutron scattering of the skyrmion lattice in MnSi using an experimental set-up that minimizes the effects of demagnetizing fields and double scattering. Under these conditions the skyrmion lattice displays resolution-limited Gaussian rocking scans that correspond to a magnetic correlation length in excess of several hundred µm. This is consistent with exceptionally well-defined long-range order. We further establish the existence of higher-order scattering, discriminating parasitic double-scattering with Renninger scans. The field and temperature dependence of the higher-order scattering arises from an interference effect. It is characteristic for the long-range crystalline nature of the skyrmion lattice as shown by simple mean field calculations.

Posters

The instruments hosted at the FRM II are operated by many groups coming from German universities, Helmholtz Research Centres and Max Planck Institutes. During the long maintenance break, the instruments and the infrastructure were improved in many different ways.

Learn all about the news by visiting the instrumentation posters!
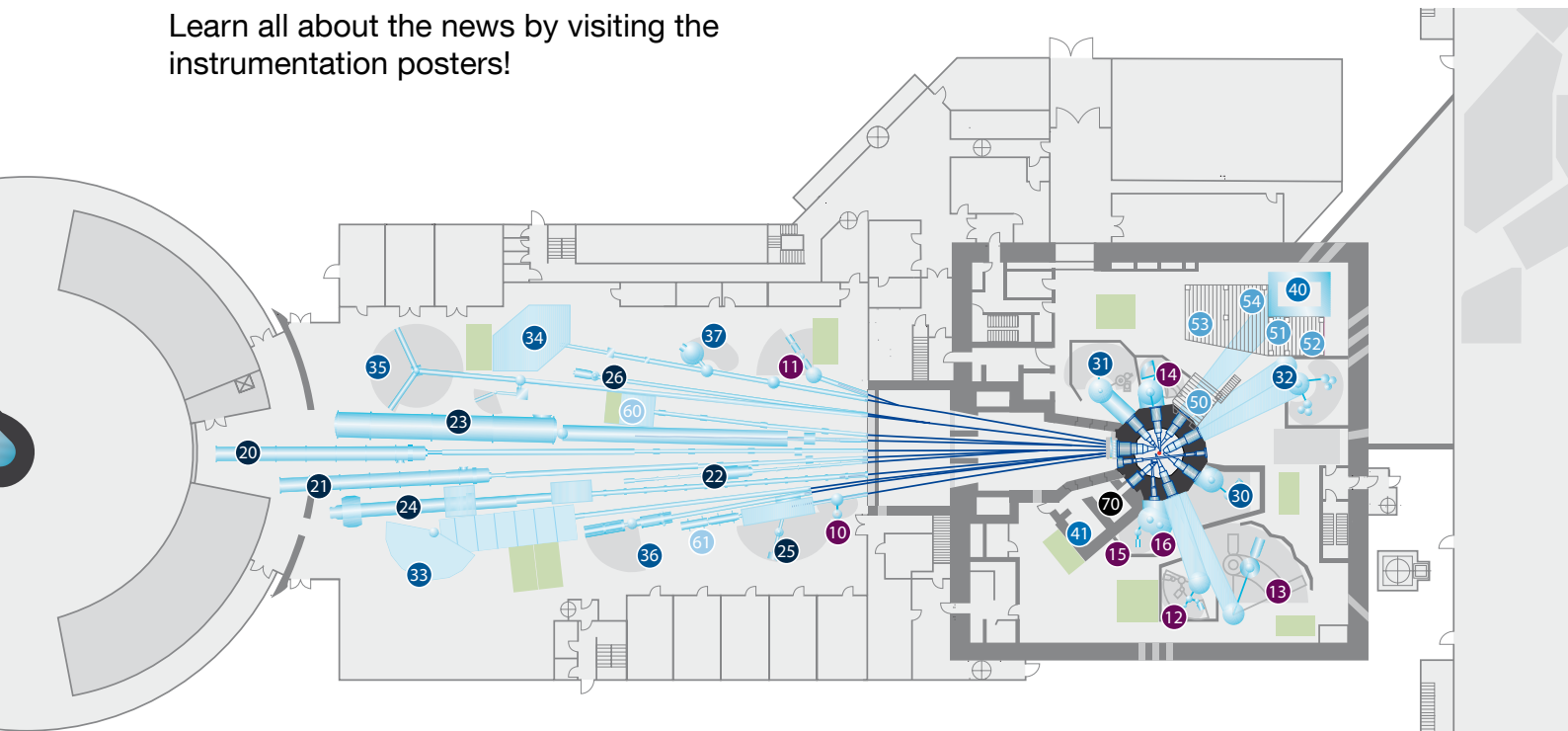
Diffraction

- (12) **RESI**
- (15) **HEIDI**
- (16) **POLI**
- (13) **SPODI**
- (14) **STRESS-SPEC**
- (10) **BIODIFF**
- (11) **MIRA**

SANS and Reflectometry

- (20) **KWS-1**
- (21) **KWS-2**
- (22) **KWS-3**
- (23) **SANS-1**
- (24) **REFSANS**
- (25) **N-REX$^+$**
- (26) **MARIA**

Spectroscopy

- (30) **PUMA**
- (31) **PANDA**
- (32) **TRISP**
- (33) **TOFTOF**
- (34) **SPHERES**
- (35) **RESEDA**
- (36) **J-NSE**
- (37) **DNS**

Imaging

- (40) **ANTARES**
- (41) **NECTAR**

Nuclear- and Particle Physics

- (60) **PGAA**
- (61) **mephisto**

Positrons

- (50) **NEPOMUC**
- (51) **CDBS**
- (52) **PAES**
- (53) **PLEPS**
- (54) **SPM**

- (70) **MEDAPP**

Do you already know our **BLUE BOOK**? There you find all information regarding the instruments at the FRM II. Just fetch you personal copy at the registration desk or order it from **userinfo@frm2.tum.de**.

BIODIFF

I-10

operated by JCNS; FRM II
Instrument team: A. Ostermann, T. Schrader

The newly built neutron single crystal diffractometer BIODIFF is a joint project of the Forschungszentum Jülich (FZJ/ JCNS) and the Forschungs-Neutronenquelle Heinz Maier-Leibnitz (FRM II). BIODIFF is especially designed to collect data from crystals with large unit cells. The main field of application is the structure analysis of proteins, especially the determination of hydrogen atom positions. For this purpose BIODIFF provides two independent detector systems.

MIRA

I-11

operated by TUM
Instrument team: G. Brandl, R. Georgii, S. Mühlbauer, R. Schwikowski

MIRA has been upgraded to perform triple axis measurements. First experiments on the spin-density wave of Cr have been performed. Results are proofing the good performance and the excellent q-resolution of the instrument in this mode. Together with the focusing guide options this allows for measurements at small samples in extreme environment like pressure, magnetic field etc.

RESI

I-12

operated by LMU; Universität Augsburg
Instrument team: B. Pedersen, G. Seidl

The design of the monochromator has been enhanced to use piezo drives with resitive encoders as feedback device. This design allows faster (1 day vs 1 week) and better alignment of the monochromator. The better alignment results in a 20 % flux increase for the Cu-422 monochromator.

STRESS-SPEC

I-14

operated by TU Clausthal; HZG; TUM
Instrument team: W. Gan, M. Hofmann, C. Randau, J. Rebelo-Kornmeier, G. Seidl

STRESS-Spec is a high flux neutron diffractometer for material science. It offers a flexible instrument set up suitable for fast residual strain and texture measurements. Recently new sample handling equipment was commissioned: E.g. a robot system allows automatic and precise sample change and depositioning for global texture and residual strain analysis. Therefore and together with a new large PSD detector the beam time can be used more efficiently.

HEIDI

I-15

operated by JCNS
Instrument team: W. Luberstetter, M. Meven, A. Sazonov

The single crystal diffractometer HEiDi was designed as a flexible tool for detailed studies on structural and magnetic properties of single crystals. HEiDi uses fast neutrons from the hot source of the Forschungs-Neutronenquelle Heinz Maier-Leibnitz (FRM II) to offer a high neutron flux in the wavelength range between 1.1 Å and 0.4 Å.

POLI

I-16

operated by JCNS
Instrument team: V. Hutanu, A. Kobba, W. Luberstetter, M. Meven

The diffractometer POLI (Polarisation Investigator) is dedicated to the investigation of single crystalline samples with complex magnetic structures using neutron spin polarisation. Spherical neutron Polarimetry (SNP) using third generation polarimeter Cryopad has been recently implemented on POLI@HEiDi. SNP is a powerful technique which permit to distinguish between the depolarisation and polarisation rotation occurred by the polarised neutron scattering.

Posters

KWS-1

operated by JCNS
Instrument team: M. S. Appavou, Z. Di, A. Feoktystov, H. Frielinghaus

KWS-1 - a high flux, high resolution SANS instrument, with higher default resolution than KWS-2 and the intensity comparable to other high-end SANS instruments in the world – serves many fields from soft to hard matter science. A high precision sample stage for heavy loads (hexapod) allows for SANS under grazing incidence (GISANS) and supports investigations of thin films. Dedicated sample environment, such as rheometers, non-magnetic pressure cells, magnets allow for studies of polymers, biological molecules, nanocomposites, colloids, complex fluids, surfactants, thin (magnetic) films, magnetic and domains structures.

KWS-2

operated by JCNS
Instrument team: V. Pipich, A. Radulescu, N. Székely

After the shut-down of the FRJ-2 "DIDO" research reactor in Jülich, the small-angle neutron diffractometer KWS-2 has been rebuilt by the Jülich Centre for Neutron Science (JCNS) at the neutron source Heinz Maier-Leibnitz (FRM II) in Garching. The instrument is 42 m long and based on the pinhole concept: the exploration of a wide momentum transfers Q, between $6x10^{-4}$ and 0.5 $Å^{-1}$, is possible by the variation of the sample-to-detector distance between 1 m and 20 m and of the wavelength between 4.5 Å and 20 Å.

KWS-3

operated by JCNS
Instrument team: Z. Fu, H. Frielinghaus, D. Korolkov, V. Pipich

KWS-3 is a very small anle neutron scattering (VSANS) diffractometer with focusing mirror, operated by the JCNS at the research neutron source Heinz Maier-Leibnitz (FRM II) at Garching. At present, the most attention is paid to the optimization of the USERBILITY (= user + usability) of KWS-3: the minimization of the required sample volume, the use of standard SANS cells and sample environment. The integration of the flexible and user friendly instrument control framework (PyFrid) as well as the data treatment software (QtiKWS), whih is common to all JCNS SANS instruments, at KWS-3 has significantly simplified instrument operation. Now, VSANS at KWS-3 is as easy as SANS. Welcome!

SANS-1

operated by HZG; TUM
Instrument team: R. Gilles, A. Heinemann, T. Heller, S. Semecky

This contribution presents the status of the new small angle neutron scattering instrument SANS-1 a common project of the TUM and the Helmholtz-Zentrum Geesthacht. The installation of the selector tower with three eligible positions for the two selectors (high resolution or high intensity) for a neutron guide is completed. The four tracks of the collimation system including a) apertures, b) neutron guides, c) background apertures, and d) a laser adjustment apparatus are aligned. Two V-shaped polarizers, a spin flipper and the guide field for polarized neutrons are installed, too.

REFSANS

operated by HZG
Instrument team: M. Haese-Seiller, J.-F. Moulin, M. Pomm

The TOF horizontal reflectometer REFSANS was initially designed by the Helmholtz Research Centre Geesthacht (now HZG, until 2011 GKSS) to study soft matter surfaces and interfaces. However it quickly appeared that this instrument is attractive to a much wider scientific community. Examples cover specular reflectometry and GISANS (in-plane resolved off-specular) measurements on biological samples, polymer thin films, hybrid polymer/inorganic materials, and metallic multi layers.

NREX

operated by Max-Planck-Gesellschaft
Instrument team: T. Keller, Y. Khaydukov, O. Soltwedel

The neutron/X-ray contrast reflectometer situated on the cold source of the research neutron source FRM II provides various grazing incidence techniques like reflectometry, grazing incidence small angle scattering/diffraction etc both in polarized and non-polarized modes. These techniques can be employed for the study of different phenomena in low-dimensional structures (surfaces, interfaces, thin layers, heterostructures etc).

MARIA

operated by JCNS
Instrument team: E. Babcock, S. Mattauch, D. Korolkov

I-26

The JCNS has installed the new, high-intensity reflectometer MARIA in the neutron guide hall of the FRM II reactor in Garching. This instrument uses a velocity selector for the monochromatization of the neutron beam, an elliptically focussing guide to increase the flux at the sample position and a double-reflecting supermirror polarizer to polarize the entire cross-section of the beam delivered by the neutron guide.
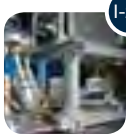
PUMA

operated by Georg-August-Universität Göttingen; TUM
Instrument team: N. Jünke, O. Sobolev, A. Teichert

I-30

The thermal triple axis spectrometer PUMA is operated by the Universität Göttingen in cooperation with the Technische Universität München. It belongs to the most powerful and flexible instruments of this type worldwide. PUMA is characterized by most efficient utilization of the available neutron flux making use of focusing techniques. Special equipment allows time-resolved experiments down to a 1µs time scale. A multianalyser/-detector system can simultaneously accept a scattering angle range of 16 degrees, so that flexible Q-ω pathways can be realized without the need of repositioning the instrument.

PANDA

operated by HZB; Technische Universität Dresden
Instrument team: E. Faulhaber, A. Schneidewind, F. Stoica

I-31

Panda is a cold three axis spectrometer for high neutron intensity. The measurements provide high resolution with high intensity for studies of magnetic excitation.

PANDA camera

operated by HZB; Technische Universität Dresden
Instrument team: E. Faulhaber, A. Schneidewind, F, Stoica

I-31a

A simple neutron camera will immediately create images on a monitor. By this a quick overview of the beam is provided.
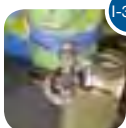
TRISP

operated by Max-Planck Society
Instrument team: T. Keller

I-32

The TRISP spectrometer at the FRM II is based on the resonance spin-echo technique (NRSE) invented by Golub and Gähler and applies the spin echo phonon focusing proposed by Mezei. Linewidths of dispersive excitations with energies up to 50 meV can be measured with a resolution in the µeV-range. We will review recent results on the momentum resolved electron-phonon interaction in elemental superconductors. The instrument also incorporates Rekveldt's Larmor diffraction technique.

TOFTOF

operated by TUM
Instrument team: W. Lohstroh, J. Ringe, G. Simeoni

I-33

TOFTOF is a cold neutron time-of-flight spectrometer suitable for both inelastic and quasi-elastic neutron scattering. It represents a quite versatile instrument, known for its excellent signal-to-background ratio as well as high energy resolution and high neutron flux. During the last long break, the instrument experienced an overall technical maintenance and a considerable upgrade of both the primary and the secondary spectrometer. The detector capacity of the fligh chamber had been increased from 605 to 1000 detectors.

Posters

SPHERES
operated by JCNS
Instrument team: G. J. Schneider, J. Wuttke, M. Zamponi

The high energy resolution spectrometer SPHERES is a third-generation backscattering spectrometer with focusing optics and a phase-space-transform chopper. It combines the high resolution with a very good signal-to-noise ratio. It is a versatile spectrometer for investigating atomic and molecular dynamics on a GHz scale. Typical applications include hyperfine splitting in magnetic materials, molecular rotations, diffusion and relaxation processes in various systems.

RESEDA
operated by TUM
Instrument team: R. Bierbaum, W. Häußler

The neutron spin-echo NSE method is based on the analysis of the intermediate scattering function, which is obtained by measuring the dependency of the polarisation on spin echo time. Thus, one of the crucial parameters in the instrument performance is the polarisation of the initial neutron beam. In this contribution we present the performance of the V-cavity-polariser of the spin-echo spectrometer RESEDA, FRM II. A good agreement is observed by the comparison of experimental results and the polarisation predicted by simulations with McStas, which is based on the Monte-Carlo method. In addition, we report on results of McStas simulations of a new compact V-cavity-polariser, which is optionally installed just before the sample position of RESEDA.
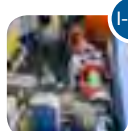
J-NSE
operated by JCNS
Instrument team: O. Holderer

The neutron spin echo spectrometer J-NSE serves to investigate slow motions on time- and lengthscales relevant for observing thermal fluctuations in mesoscopic systems. With its high energy resolution, low background and good instrmental stability it was possible to tackle also scientific questions where scattering from the sample is extremely small, as e.g. under grazing incidence conditions.

DNS
operated by JCNS
Instrument team: Y. Su

DNS is a cold neutron diffuse scattering spectrometer with polarization analysis at the neutron guide NL6a, FRM II. With its compact design, large double-focusing PG(002) monochromator and efficient supermirror-based polarizer and polarization analyzers, DNS is optimized as a high intensity instrument. A polarized neutron flux in the range of 10^7 n/(s×cm^2) in the cold neutron regime and a polarization rate as high as 96% can be routinely obtained. A large-array position sensitive detectors (PSD) covering 1.9 sr and a high-frequency double-disc chopper system are being developed at DNS.

ANTARES
operated by TUM
Instrument team: B. Schillinger, P. Schmakat, M. Schulz, P. Torrigo

As the old ANTARES beam line SR4b is the only cold beam line that can be extended to the new Eastern Guide Hall, ANTARES had to be completely dismantled and rebuilt at the neighboring beam channel SR4a. ANTARES Upgrade will be commissioned in spring/summer 2012 and will, in addition to nearly identical possible parameters as the old ANTARES, offer many extended new capabilities, such as a second experimental chamber closer to the reactor for higher flux, and six instead of two selectable collimators for higher flux or higher resolution.

NECTAR
operated by TUM
Instrument team: T. Bücherl

The radiography and tomography facility NECTAR is using fission neutrons with a mean energy of about 1.9 MeV for the non-destructive investigation of bulky objects. As dense materials like iron, lead etc. can easily be penetrated by these neutrons while being sensitive to hydrogen, NECTAR is well suited for the investigations of technical, art historical, biological and geological samples.
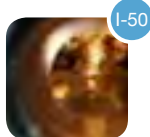
NEPOMUC
I-50

operated by Universität der Bundeswehr München; TUM
Instrument team: H. Ceeh, W. Egger, C. Hugenschmidt, C. Piochacz

The neutron induced positron source NEPOMUC at the FRM II has been replaced by a new beam tube in order to provide a high intensity of moderated positrons. The high positron intensity leads not only to a drastically reduced measurement time and an improved signal-to-noise ratio but also to the realization of new experiments using mono-energetic positrons.

PGAA
I-60

operated by Universität zu Köln; PSI
Instrument team: L. Canella, P. Kudejova, S. Söllradl, Z. Revay

Prompt Gamma Activation Analysis (PGAA) is a nuclear analytical technique for the determination of elemental composition of samples. Because of the deep penetration of both neutron and gamma radiation the method provides the average composition of the whole irradiated volume. It is mainly used for the analysis of major and minor components of the materials, and it is especially useful for the investigation of light elements, first of all H and B. The PGAA facility at Garching has been rebuilt so that the background-to-signal ratio makes possible the most sensitive measurements, and in the high flux-beam, extremely low-mass samples (below 1 mg) can be analyzed, too.
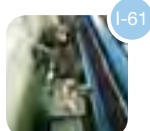
MEPHISTO
I-61

operated by TUM
Instrument team: J. Klenke, K. Lehmann, H. Saul

The experimental area MEPHISTO, dedicated to experiments in the field of particle and nuclear physics will move in the near future. It will use the new neutron guide which will be extended to the new neutron guide hall east. The guide is a m=2.5, single curved, 60x106 mm^2 cold neutron guide. It is optimised for PERC, the first experiment at the new MEPHISTO. It is already planned to install a secondary spectrometer which uses the source PERC to investigate aspects of the free neutron decay and its products.

Neutron Guides at FRM II
I-71

C. Breunig, E. Kahle, A. Kriele, P. Link, J. Weber (all FRM II)
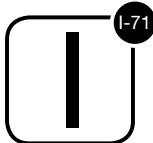
As one of our main suppliers for precision glass cutting and gluing ceased production, we decided to take over the fabrication of neutron guides ourselves. We established a laboratory close to our sputtering facility and equipped it with all necessary tools to machine the glass and glue it together accurately after sputtering, while optically controlling the shape. We constructed and assembled a special glass sawing facility for cutting, grooving and phasing. The first neutron guides were produced successfully, demonstrating a state-of-the-art performance. This enables us to respond quickly to sudden needs and the special requirements of the instruments at FRM II.

Sample Environment FRM II
I-72

H. Kolb, J. Peters, H. Weiß (all FRM II)

Beside state of the art neutron scattering instrumentation, sample environment is an other important pillar to attract the user community. Some new available devices and developments are presented like close cycle refrigerators with temperature extension down to1.3 K or high pressure equipment. Furthermore the User Meeting is very convenient for the interchange and discussion amongst users and central groups to initiate new developments.

Sample Environment JCNS
I-73

H. Schneider, D. Vujevic (all JCNS)
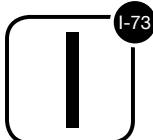
The JCNS sample environment is dedicated to hard and soft matter applications on JCNS instruments at the JCNS outpost at the FRM II.

Posters
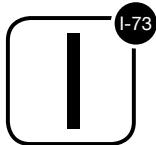
NICOS (upcoming)
*G. Brandl (FRM II), E. Faulhaber (TU Dresden), J. Krüger (FRM II), B. Pedersen (FRM II),
A. Schneidewind (HZB)*

NICOS („Networked Instrument COntrol System"), almost completely written in Python, is the upcoming standard instrument control software at the FRM II. The advantages of NICOS are quick integration of additional equipment into the software control, easy use, specific user interfaces for different instruments, a full set of standard commands for all instruments, and flexibility for uncommon experiments due to full access to the Python language. At the moment NICOS is in operation at: PANDA, PUMA, RESI, MIRA, REFSANS, and TOFTOF. PGAA as well as ANTARES will follow soon.
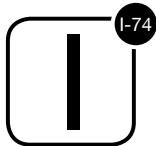
HELIOS
S. Masalovich (FRM II)

The optical pumping facility HELIOS for a large-scale production of a dense spin-polarized ^{3}He gas as well as an application of neutron spin filters (NSF) at FRM II are presented. ^{3}He NSFs make a great impact on the instrumentation for neutron polarization and polarization analysis since polarized nuclei of ^{3}He possess very high spin-dependent neutron absorption efficiency over a wide range of neutron energies. The straight-line passage of a neutron beam through a NSF with no change of a neutron trajectory enables one to measure a neutron polarization for nearly any divergent scattered beam.
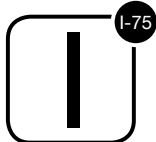
EDM
G. Petzold (TUM) for the nEDM project

A non-zero value of an electric dipole moment (EDM) of a fundamental system would be a clear indication of time reversal symmetry (T) violation and, under the assumption that the combined operation of CPT is conserved, CP violation. Due to its simple structure, the free neutron is one of the most suitable systems to search for an EDM. The goal of next generation experiments that are currently being planned all over the world is an improvement of the sensitivity by 1-2 orders of magnitude into the 10^{-28} ecm regime, probing scales beyond the reach of the LHC at CERN. We are currently setting up one such experiment at the FRM II research neutron source at Garching.
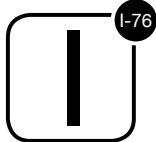
PERC
B. Märkisch (Universität Heidelberg) for the PERC collaboration

The PERC collaboration will perform high-precision measurements of angular correlations in neutron beta decay at the beam facility MEPHISTO. The new beam station PERC, a clean, bright, and versatile source of neutron decay products, is designed to improve the sensitivity of neutron decay studies by one order of magnitude. The charged decay products are collected by a strong longitudinal magnetic field directly from inside a neutron guide. This combination provides the highest phase space density of decay products. A magnetic mirror serves to perform precise cuts in phase space, reducing related systematic errors.

Index

Index

List of Participants

Adams Tim	tim.adams@frm2.tum.de	TUM
Alhamdany Nowfal	nowfal.alhamdany@tu-clausthal.de	TU Clausthal @ FRM II
Appavou Marie-Sousai	m.s.appavou@fz-juelich.de	JCNS
Beimler Alexander	Alexander.Beimler@frm2.tum.de	FRM II
Blanchard Didier	didier.blanchard@risoe.dk	DTU-Energy Conversion
Böni Peter	pboeni@frm2.tum.de	TUM
Brandl Georg	georg.brandl@frm2.tum.de	FRM II
Breunig Christian	christian.breunig@frm2.tum.de	FRM II
Bücherl Thomas	thomas.buecherl@tum.de	FRM II
Calzada Elbio	elbio.calzada@frm2.tum.de	FRM II
Canella Lea	Lea.Canella@frm2.tum.de	FRM II
Carsughi Flavio	f.carsughi@fz-juelich.de	JCNS
Chatterji Tapan	chatterji@ill.fr	ILL
Cristiano Fernando	Fernando.Cristiano@frm2.tum.de	FRM II
Di Zhenyu	z.di@fz-juelich.de	JCNS
Ener Semih	semih.ener@tum.de	TUM
Faulhaber Enrico	enrico.faulhaber@helmholtz-berlin.de	HZB
Feoktystov Artem	a.feoktystov@fz-juelich.de	JCNS
Frei Andreas	andreas.frei@tum.de	FRM II
Frielinghaus Henrich	h.frielinghaus@fz-juelich.de	JCNS
Gan Weimin	weimin.gan@hzg.de	HZG
Gilles Ralph	ralph.gilles@frm2.tum.de	TUM
Glomann Thomas	t.glomann@fz-juelich.de	JCNS
Gold Barbara	b.gold@fz-juelich.de	JCNS
Haunholter Axel	axel.haunholter@frm2.tum.de	TU Dresden
Häußler Wolfgang	wolfgang.haeussler@frm2.tum.de	TUM
Hertrich Samira	samira.hertrich@physik.lmu.de	LMU
Hess Kai-Uwe	hess@lmu.de	LMU
Hesse Connie	Connie.Hesse@frm2.tum.de	FRM II
Hilbig Harald	hilbig@cbm.bv.tum.de	TUM
Hoelzel Markus	markus.hoelzel@frm2.tum.de	FRM II
Hofmann Michael	michael.hofmann@frm2.tum.de	FRM II
Holderer Olaf	o.holderer@fz-juelich.de	JCNS
Hopfenmüller Bernhard	b.hopfenmueller@fz-juelich.de	JCNS
Hugenschmidt Christoph	hugen@frm2.tum.de	FRM II
Hutanu Vladimir	vladimir.hutanu@frm2.tum.de	RWTH Aachen
Ioffe Alexander	a.ioffe@fz-juelich.de	JCNS
Iyudin Anatoli	ani@mpe.mpg.de	Skobeltsyn Institute of Nuclear Physics
Jaksch Sebastian	sebastian.jaksch@tum.de	TUM
Keller Thomas	Thomas.Keller@frm2.tum.de	MPI für Festkörperforschung
Khaydukov Yury	Yury.Khaydukov@frm2.tum.de	MPI für Festkörperforschung

List of Participants

Klenke Jens	jens.klenke@frm2.tum.de	FRM II
Krakovský Ivan	ivank@kmf.troja.mff.cuni.cz	Charles University Prague
Krüger Jens	jens.krueger@frm2.tum.de	FRM II
Kudejova Petra	Petra.Kudejova@frm2.tum.de	FRM II
Link Peter	peter.link@frm2.tum.de	FRM II
Lipfert Frederik	f.lipfert@fz-juelich.de	FRM II
Liu Shuquan	liushuquan@pku.edu.cn	Peking University
Lohstroh Wiebke	wiebke.lohstroh@frm2.tum.de	FRM II
Lott Dieter	dieter.lott@hzg.de	HZG
Masalovich Sergey	sergey.masalovich@frm2.tum.de	FRM II
Mattauch Stefan	s.mattauch@fz-juelich.de	JCNS
Metwalli Ezzeldin	ezzmet@ph.tum.de	TUM
Meven Martin	martin.meven@frm2.tum.de	FRM II
Moulin Jean-Francois	jean-francois.moulin@hzg.de	HZG @ FRM II
Mühlbauer Sebastian	Sebastian.Muehlbauer@frm2.tum.de	FRM II
Mukherji Debashis	d.mukherji@tu-bs.de	TU Braunschweig
Müller-Buschbaum Peter	muellerb@ph.tum.de	TUM
Nagy Béla	nagyb@rmki.kfki.hu	Wigner Research Centre
Nakagawa Hiroshi	h.nakagawa@fz-juelich.de	JCNS
Neuhaus Jürgen	juergen.neuhaus@frm2.tum.de	FRM II
Nickel Bert	nickel@lmu.de	LMU
Niedermeier Martin	niedermeier.martin@ph.tum.de	TUM
Nowak Gregor	gregor.nowak@rub.de	HZG
Ostermann Andreas	andreas.ostermann@frm2.tum.de	FRM II
Papadakis Christine	papadakis@tum.de	TUM
Paul Amitesh	amitesh.paul@frm2.tum.de	TUM
Paul Neelima	neelima.paul@helmholtz-berlin.de	TUM
Pedersen Bjørn	bjoern.pedersen@frm2.tum.de	FRM II
Peters Jürgen	juergen.peters@frm2.tum.de	FRM II
Petzoldt Gerd	petzoldt@tum.de	TUM
Philipp Martine	martine.philipp@tum.de	TUM
Pipich Vitaliy	v.pipich@fz-juelich.de	JCNS
Radulescu Aurel	a.radulescu@fz-juelich.de	JCNS
Rawolle Monika	monika.rawolle@ph.tum.de	TUM
Rebelo-Kornmeier Joana	Joana.Kornmeier@frm2.tum.de	FRM II
Reihle Matthias	mre@utg.de	TUM
Repper Julia	julia.repper@psi.ch	PSI
Révay Zsolt	zsolt.revay@frm2.tum.de	FRM II
Rolph James	james.rolph@postgrad.manchester.ac.uk	University of Manchester
Roosen-Runge Felix	feroru@gmx.de	Universität Tübingen
Saul Heiko	Heiko.Saul@frm2.tum.de	FRM II
Schillinger Burkhard	burkhard.schillinger@frm2.tum.de	FRM II

Schindler Markus	markus.schindler@ph.tum.de	TUM
Schmakat Philipp	philipp.schmakat@frm2.tum.de	FRM II
Schneider Gerald	g.j.schneider@fz-juelich.de	JCNS
Schneider Florian	f.schneider@fz-juelich.de	JCNS
Schneider Harald	ha.schneider@fz-juelich.de	JCNS
Schneidewind Astrid	astrid.schneidewind@frm2.tum.de	HZB @ FRM II
Schrader Tobias E.	t.schrader@fz-juelich.de	JCNS
Schulz Michael	michael.schulz@frm2.tum.de	FRM II
Senyshyn Anatoliy	senyshyn@frm2.tum.de	FRM II
Sepe Alessandro	alessandro.sepe@tum.de	TUM
Simeoni Giovanna	giovanna.simeoni@frm2.tum.de	FRM II
Solbrig Konrad	konrad.solbrig@hs-owl.de	Hochschule Ostwestfalen-Lippe
Söllradl Stefan	stefan.soellradl@frm2.tum.de	FRM II
Soltwedel Olaf	Olaf.Soltwedel@frm2.tum.de	MPI für Festkörperforschung
Spehr Tinka	Tinka.Spehr@desy.de	DESY
Stoica Florin George	florin.stoica@frm2.tum.de	HZB
Strunz Pavel	strunz@ujf.cas.cz	NPI Rez
Su Yixi	y.su@frm2.tum.de	JCNS
Szekely Noemi	n.szekely@fz-juelich.de	JCNS
Vujevic Daniel	d.vujevic@fz-juelich.de	JCNS
Wehrs Juri	j.wehrs@tu-bs.de	TU Braunschweig
Wiesmaier Sebastian	sebastian.wiesmaier@min.uni-muenchen.de	LMU
Yao Yuan	yuan.yao@ph.tum.de	TUM
Zamponi Michaela	m.zamponi@fz-juelich.de	JCNS
Zanatta Marco	zanatta@science.unitn.it	University of Trento
Zeitelhack Karl	Karl.Zeitelhack@frm2.tum.de	FRM II